

**STUDY ON DIRECT TORQUE CONTROL OF  
PERMENANT MAGNET SYNCHRONOUS  
MOTOR FOLLOWING DUTY RATIO  
MODULATION WITH ADVANCED MTPA  
SCHEME TO MINIMIZE TORQUE RIPPLE**

*A thesis is submitted to fulfil the requirement of the degree*

**Master in Electrical Engineering**

Submitted by

**TAPAS SADHUKHAN**

Examination Roll no. – **M4ELE23020**

Registration no. – **153998 of 2020-2021**

Under the guidance of

**Dr. Susanta Ray**

and

**Prof. Arabinda Das**

Electrical Engineering Department

Jadavpur University

Kolkata – 700 032

JUNE 2023

**Faculty of Engineering and Technology  
Jadavpur University, Kolkata - 700032**

**Certificate**

This is to certify that the thesis entitled “**Study on Direct Torque Control of Permanent Magnet Synchronous Motor following Duty Ratio Modulation with advanced MTPA scheme to Minimize torque ripple**”, submitted by **Mr. Tapas Sadhukhan** (Examination Roll No. M4ELE23020), under our supervision and guidance during the session of 2020-23 in the department of Electrical Engineering, Jadavpur University. We are satisfied with his work, which is being presented for the partial fulfilment of the degree of **Master in Electrical Engineering** from Jadavpur University, Kolkata-700032.

.....  
**Prof. Susanta Ray**  
Associate Professor  
Department of Electrical Engineering  
Jadavpur University  
Kolkata, 700 032

.....  
**Prof. Arabinda Das**  
Professor  
Department of Electrical Engineering  
Jadavpur University  
Kolkata, 700 032

.....  
**Prof. Ardhendu Ghoshal**  
Dean of Faculty Council of  
Engineering and Technology  
Jadavpur University  
Kolkata, 700 032

.....  
**Prof. Biswanath Roy**  
Head of the Department of  
Electrical Engineering  
Jadavpur University  
Kolkata, 700 032

**Faculty of Engineering and Technology  
Jadavpur University, Kolkata – 700 032**

**Certificate of Approval**

The forgoing thesis entitled “**Study on Direct Torque Control of Permanent Magnet Synchronous Motor following Duty Ratio Modulation with advanced MTPA scheme to Minimize torque ripple**” is hereby approved as a creditable study of an Engineering subject carried out and presented in a manner that fulfils its acceptance as a prerequisite to the degree for which it is submitted. It is understood that by this approval, the undersigned does not necessarily endorse or approve any statement made, opinion expressed, or conclusion drawn therein but approves the thesis only for the purpose for which it is submitted.

**The final examination for evaluation of the thesis**

Signature of the examiners

.....

.....

.....

## **Declaration of Originality**

I hereby declare that this thesis contains a literature survey and original research work done by me. All the information in this document has been obtained and presented according to academic rules and ethical conduct. I also declare that, as required by these rules and conduct, I have fully cited and referenced all material and results that are not original to this work.

Name: Tapas Sadhukhan

Examination Roll No : M4ELE23020

Thesis Title: Study on Some Advanced Methodologies on Direct Torque Control of Permanent Magnet Synchronous Motor for Minimizing Torque Ripple.

Signature with Date :

## ACKNOWLEDGMENTS

I express my sincere gratitude to my supervisor, **Prof. Susanta Ray** for his encouragement, suggestion and advices, without which it would not have been possible to complete my thesis successfully. I would like to thank **Prof. Arabinda Das** for being a constant source of encouragement, inspiration and for his valuable suggestions coupled with his technical expertise throughout my research work. It was a great honour for me to pursue my research under his supervision.

I would also like to thank my co-worker Mohammad Aadil Hasan, all the staffs of Drives and Simulation laboratory, and the research scholars of our department for providing constant encouragement throughout my thesis work.

Last but not the least I extend my words of gratitude to my parents for personally motivating me to carry out the work smoothly.

## ABSTRACT

This thesis studies the mathematical model of Permanent Magnet Synchronous Motor (PMSM), a general idea of the conventional Direct Torque Control (DTC) method, a DTC based on duty ratio modulation, Maximum torque per ampere (MTPA) based duty ratio modulated DTC, and advanced duty ratio modulation scheme combining previous two methods. Space Vector Modulation (SVM) is used to choose the inverter's voltage vectors for various time periods. Look-Up Table (LUT) is used to choose the voltage vectors for various values of torque and flux with various phases. The two approaches discussed above are then used to simulate the PMSM drive in the MATLAB® SIMULINK environment. Then the ripples produced in speed and torque response of DTC with duty ratio modulation, DTC with MTPA based duty ratio modulation and advanced Duty ratio modulation are compared. It is obvious that DTC has a specific drawback because of how much torque and current ripple it possesses. An efficient remedy for this problem is the Advanced Duty Ratio Modulation Technique. The advanced duty ratio modulated approach is preferred for greatly lowering the ripple percentage, according to this thesis work. When there are changes in load, it can also lower the torque ripple.

<b>Chapter No.</b>	<b>CONTENTS</b>	<b>Page No.</b>
	<b>Acknowledgment</b>	<b>5</b>
	<b>Abstract</b>	<b>6</b>
	<b>List of Acronyms</b>	<b>9</b>
	<b>List of symbols used</b>	<b>10-11</b>
	<b>List of Figures</b>	<b>12-13</b>
	<b>List of Tables</b>	<b>14</b>
<b>1</b>	<b>Introduction and Literature Review</b>	<b>15-21</b>
1.1	History of Permanent Magnets Machines	15
1.2	Motivation of Work	16
1.3	Literature Review	17
1.4	Organization of the Thesis	20
<b>2</b>	<b>Permanent Magnet Synchronous Motor</b>	<b>22-35</b>
2.1	Introduction	22
2.2	Construction Of PMSM	22
2.2.1	Rotor Construction	22
2.2.2	Stator Construction	26
2.3	Working Principle of PMSM	25
2.4	Mathematical Modelling of PMSM	27
2.4.1	Three-phase to two phase transformations (ABC to DQ)	27
2.4.2	Motor modelling	28
2.4.3	Electromagnetic Torque Equation	33
2.4.4	Mechanical system model	34
2.4.5	Final modelling equation	34
<b>3</b>	<b>Voltage Source Inverter</b>	<b>36-41</b>
3.1	Introduction	36
3.2	Power devices used in VSI	36
3.3	VSI Topology	36
3.4	Switching States of VSI	40
<b>4</b>	<b>Traditional Direct Torque Control</b>	<b>42-54</b>
4.1	Introduction	42
4.2	Working Principal of DTC	43
4.3	Controller of DTC	46
4.3.1	Flux and sector estimator	46
4.3.2	Torque Estimation	48
4.3.3	Torque and Flux hysteresis controller	48
4.3.3.1	Flux Hysteresis Controller	48
4.3.3.2	Torque Hysteresis Controller	49
4.3.4	Switching table	50

4.4	DTC Schematic	53
<b>5</b>	<b>Duty Ratio Modulation Scheme</b>	<b>55-58</b>
5.1	Preliminary Idea	55
5.2	Purpose of use	55
5.3	Application	55
5.4	Duty ratio calculation	56
<b>6</b>	<b>Maximum Torque Per Ampere Control</b>	<b>59-62</b>
6.1	Basic Principle Of MTPA	59
6.1.1	Field Weakening Control	59
6.1.2	MTPA	60
6.2	Control Action	61
<b>7</b>	<b>Advanced Duty ratio Modulation Scheme</b>	<b>63-65</b>
7.1	Basic Principle	63
7.2	Proposed Method	63
<b>8</b>	<b>Results and Discussion</b>	<b>66-74</b>
8.1	Simulation	66
8.1.1	Block Diagrams developed in Simulink	67
8.2	Results	69
8.2.1	Speed Response	69
8.2.2	Torque Response	71
8.2.3	Observation	73
8.3	Comparison of the results and discussion	73
<b>9</b>	<b>Conclusion</b>	<b>75-76</b>
9.1	Contributions to the work	75
9.2	Scopes of the future work	76
	<b>Appendix</b>	<b>77</b>
	<b>References</b>	<b>78-82</b>



## List of Acronyms

Short Form	Full-Form
DC	Direct Current
PM	Permanent Magnet
AC	Alternating Current
PMSM	Permanent Magnet Synchronous Motor.
SCR	Silicon-Controlled Rectifier
EMF	Electro Motive Force
D-Q	Direct-Quadrature
FOC	Field Oriented Control
DTC	Direct Torque Control
LUT	Look-Up Table
PWM	Pulse Width Modulation
IM	Induction Motor
SVM	Space Vector Modulation
MTPA	Maximum Torque Per Ampere
SPM	Surface mounted Permanent Magnet
SIPM	Surface inset Permanent Magnet
IPM	Interior Permanent Magnet
MMF	Magneto Motive Force
SV-PWM	Space Vector- Pulse Width Modulation
PI	Proportional Integral
SPMSM	Surface Mounted Permanent Magnet Synchronous Machine
VSI	Voltage Source Inverter
GTO	Gate Turn off Thyristor
BJT	Bipolar Junction Transistor
MOSFET	Metal Oxide Semiconductor Field Effect Transistor
IGBT	Insulated Gate Bipolar Junction Transistor

## List of Symbols

Symbols	Meaning
$N_s$	Synchronous Speed
$f$	Frequency
$P$	Pole Pair
$\theta_r$	Angle between rotor reference frame and fixed stator axis
$L_d$	Inductance along D-axis
$L_q$	Inductance along Q-axis.
$v_q, v_d$	Stator Voltages Along Q and D axis
$v_a, v_b, v_c$	Stator Voltage along A, B and C axis
$\Psi_r$	Rotor Flux
$\Psi_a, \Psi_b, \Psi_c$	Stator Flux Along A, B and C axis
$\Psi_d, \Psi_q$	Stator Flux Along D and Q axis
$L_{kk}$	Self-inductance of the $k$ -th phase
$L_{ij}$	Mutual inductance of $i$ -th phase due to $j$ -th phase
$i_a, i_b, i_c$	Stator current along A, B and C axis
$i_d, i_q$	Stator current along D and Q axis
$R_s$	Stator Resistance
$\omega_s$	Stator Synchronous Speed
$P_{in}$	Input Power
$P_{out}$	Output Power
$H_T$	Torque Hysteresis Limit
$t_k$	On Time
$t_0$	Off Time
$T_H$	Torque Hysteresis Bandwidth
$\Delta T_m$	Torque Error
$S_A, S_B, S_C$	Switching Pulse of Leg, A, B and C of Voltage Source Inverter
$\psi^s$	Stator Flux
$\delta$	Load Angle
$i_\alpha, i_\beta$	Stator current along $\alpha$ and $\beta$
$v_\alpha, v_\beta$	Stator voltage along $\alpha$ and $\beta$
$\alpha$	The angle between two components of stator flux vector
$\psi_{ref}$	Reference Flux
$\psi_{err}$	Flux Error
$H_\psi$	Flux Hysteresis Limit

$T_s$	Sample Time
$d$	Duty Ratio
$T_e$	Electro-Magnetic Torque
$T_L$	Load Torque
$J$	Moment Of Inertia
$B$	Viscous Co-efficient
$\omega_r$	Rotor Speed

## List of Figures

No.	Figures	Page No.
2.1	Comparison between cylindrical rotor and Salient pole Synchronous machine	23
2.2	a) Distributed windings. (b) Concentrated windings	26
2.3	Motor Axis	29
2.4	(a) D-axis circuit and (b) Q-axis circuit	33
2.5	Simulink Based Model of PMSM	35
3.1	Topology of Voltage source inverter	37
3.2	Phase voltages for 180-degree conduction mode	38
3.3	The Resultant Voltage Vector of the Switching Status (1, 0, 0)	40
3.5	Inverter Eight Voltage Vectors in D-Q plane	41
4.1	Schematic Diagram of Conventional Direct Torque Control	43
4.2	Voltage vectors and the six sectors for stator flux	44
4.3	Stator and rotor flux in D-Q reference frame	45
4.4	The Flux Comparator	49
4.5	The Torque Comparator	50
4.6	Different potential switching voltage vectors and the location of the stator flux vector.	51
4.7	Potential stator flux vector paths with DTC inside the hysteresis band	53
4.8	Direct Torque Control Schematic Diagram	54
5.1	Duty Ratio Modulation	56
5.2	The comparisons of switching signals and torque waveform	57
5.3	Duty Ratio Modulated Direct Torque Control	58
6.1	Field Weakening Control Plot	59
6.2	MTPA Curve	60
7.1	Schematic Diagram of Modified DTC	65
8.1	Simulink Block Diagram for conventional DTC of PMSM	67
8.2	Simulink Block Diagram for Duty ratio modulated DTC of PMSM	68
8.3	Simulink Block Diagram for Advance Duty ratio modulated DTC of PMSM	68
8.4	Simulation Result of Speed Response of Conventional-DTC	69
8.5	Simulation Result of Speed Response of Duty Ratio Modulated DTC	69
8.6	Simulation Result of Speed Response of MTPA based Duty Ratio Modulated DTC	70
8.7	Simulation Result of Speed Response of Advance Duty Ratio Modulated DTC	70
8.8	Simulation Result of Torque Response of Conventional-DTC	71
8.9	Simulation Result of Torque Response of Duty Ratio Modulated DTC	71

8.10	Simulation Result of Torque Response of MTPA based Duty Ratio Modulated DTC	72
8.11	Simulation Result of Torque Response of Advanced Duty Ratio Modulated DTC	72

## **List of Tables**

<b>No.</b>	<b>Tables</b>	<b>Page No.</b>
3.1	Switching state of 3-phase Voltage source inverter	37
4.1	Sector selection table	50
4.2	General Selection Table for Direct Torque Control, (n=sector)	55
4.3	Voltage Vector Selection Table for Direct Torque Control	55
8.1	PMSM Parameter	69
8.2	Comparison of results and Discussion	76
	<b>Appendix</b>	80

# Chapter 1

## Introduction and Literature Review

Permanent Magnet Synchronous Motor is one that incorporates permanent magnets within the steel rotor in order to generate a magnetic field that is continuous. This motor is ideal for a wide range of motion control applications.

Stator windings connected to a 3-Phase AC source generates a rotating magnetic field. After that, the rotor poles align themselves in synchronous motion with the rotating magnetic field. The most frequent magnets utilised in these motors are neodymium magnets.

### **1.1 History of Permanent Magnets Machines:**

The development of DC machines with Permanent Magnet field excitation began in the 1950s as a result of the availability of contemporary permanent magnets with a high energy density. DC machines were finally created as a result of the use of permanent magnets (PMs) to replace electromagnetic poles with windings that needed a source of electric energy. Similar to this, brush assemblies and slip rings are not required in synchronous machines because the PM poles in the rotor replace the conventional electromagnetic field poles [3].

The mechanical commutator was replaced with an electronic commutator in the form of an inverter with the introduction of power electronic transistors and silicon-controlled rectifier devices in the late 1950s. PMSMs were developed as a result of these two advancements. If the mechanical commutator is replaced by an electronic equivalent, the armature of the dc machine does not need to be on the rotor. As a result, the machine's armature may be mounted upon the stator, allowing for greater cooling and higher voltages due to the stator's large clearance room for insulation. These machines are basic examples of what is known as "an inside out dc machine,"

in which the field and armature are reversed, moving from the stator to the rotor and then from the rotor to the stator, respectively [3] [24].

The rotor of PMSM provides a constant magnetic field, but it requires a variable magnetic field to start, hence these motors need a variable frequency power supply. Permanent magnet synchronous motors require a driver to function; they cannot function without one [24].

Since the back EMF of the PMSM is sinusoidal, sinusoidal stator currents are required to keep the torque constant. PMSM is virtually identical to a wound rotor synchronous machine, with the two primary distinctions being that the PMSMs often lack damper windings and rely on a permanent magnet for excitation instead of a field winding. D-Q mathematical model of PMSM was constructed from Synchronous Motor model using this theory, by omitting equations of damper winding dynamics and field current dynamics. This model was first proposed by R. Krishnan and P. Pillay; in 1988 [1].

## **1.2 Motivation of Work:**

Due to its several advantages Permanent magnet synchronous motor drives are replacing the traditional Induction motor and dc motor drives and becoming popular in most of the industries

The main drawback for PMSM is speed control. Since there is only one source – the AC supply that is on the stator – controlling the AC supply that is on the stator is the only way to regulate this motor. For this, a complex control system including power electronics and microcontrollers is required.

In the latter half of the 1950s, technological advancements led to the creation of new devices that were based on the switching power transistor and silicon-controlled rectifiers, after this many control techniques were proposed but most common and popular two techniques are FOC(Field Oriented Control) and DTC(Direct Torque Control). After comparing between DTC and FOC we can see DTC, unlike FOC, does



not need the use of a current regulator, coordinate transformation, or a PWM signal generator. Beside of its simplicity it provides extremely high dynamic torque response. Furthermore, in compared to FOC, Direct torque controller is less sensitive to machine parameters. Only stator resistance is required to implement this type of control [4].

Despite of its many advantages one major drawback of DTC is high torque and current ripple. In this thesis an advance duty ratio control based DTC technique is proposed to reduce torque ripple. Prime task of this process is to determine the duty ratio. The motive of this work is to propose a technique which can reduce the torque ripple more effectively than the conventionally used technique. Also, a simulation in MATLAB Simulink platform has been carried out to prove the effectiveness of this model.

### **1.3 Literature Review:**

Induction motors were being used extensively on many industries due to its robustness and advancement of AC drive system. Also, the absence of brushes, commutators, and slip rings makes the motor cheaper and maintenance free. But major drawback of this machine is lower efficiency and power to weight ratio.

In order to address this issue, PMSM drives were invented in the 1950s. Due to their many structural and functional characteristics, such as their ability to operate at a variety of speeds, PMSM are currently replacing IM drives in industries such as machine positioning, robotics, electric and hybrid cars, aeronautical systems, etc. 1) greater efficiency compared to IM since it produces less heat 2) lower size results in increased power density, 3). lower cost of maintenance due to emission of brushes, 4). higher torque-to-current ratio. 5). higher power factor [3].

But one major challenge for PMSM drives was controlling its speed there was many techniques to control the speed of AC drives like Variable frequency SCR inverter with auxiliary current circuit and feedback current transformer [5]. Also, there is a technique where Pulse Width Modulated Inverters are used to obtain variable

frequency-variable voltage [6]. But all these techniques were less efficient and decoupling between flux and electromagnetic torque does not exist in those technique.

In order to get a decoupled control between flux and electromagnetic torque DTC was first introduced by I. Takahashi and T. Noguchi, in 1986 [7]. The findings of this paper shows that this control method has outstanding torque response and efficiency characteristics, proving its validity with a simpler structure. After that a High-Performance Direct Torque Control method was proposed by I. Takahashi and Y. Ohmori [8]. In this method the torque response of the system was improved by using two sets of three-phase inverters. Instantaneous voltage vectors applied by an inverter give some degree of flexibility in determining the switching modes of a power converter. High-speed torque control and main flux management are made possible via the use of this switching flexibility. T. G. Habetler and D. M. Divan followed their work and proposed a direct torque control scheme using discrete pulse-modulated inverters [9]. The use of only one current sensor in the DC connection makes this control mechanism is unique. H. Y. Zhong, H. P. Messinger and M. H. Rashad made some further improvement in this field and proposed a microcomputer-based direct primary flux and torque control system [10]. Using a non-zero space voltage vector and its time breadth, they demonstrated that the main flux amplitude could be modified, as could the electromagnetic torque amplitude. Over the time many other DTC techniques were proposed like DTC using space vector modulation, DTC using PWM inverter [11]-[12]. In 1997 DTC was first investigated on PMSM by L. Zhong, M. F. Rahman *et al.* They used mathematics to demonstrate that the increase in electromagnetic torque in a permanent magnet motor is proportional to the increase in angle between the stator and rotor flux linkages. As a result, they demonstrated that the rapid torque response could be achieved by modifying the rotational speed of the stator flux linkage in the shortest amount of time possible. It is also proved that zero voltage vectors should not be used, and that the stator flux linkage should always be moving in proportion to the rotor flux linkage. Both of these findings are supported by the evidence presented here [13]. The conventional direct torque control does not require any motor parameter except the stator resistance. Using this flux and

Electromagnetic torque are estimated and compared with reference value. Also, two hysteresis controllers are used here the according to the output of these two controller and position of flux vector an appropriate voltage vector is selected from a switching table according to the voltage vector the switching state of the inverter is selected. In 1999 [14] L. Zhong, M. F. Rahman *et al.* implemented their investigation of DTC on a prototype PMSM which has a standard induction motor stator. They also derived the switching table specific for an interior PMSM.

Out of few drawbacks one of the major drawbacks in DTC of PMSM is torque ripple. In order to solve this problem several techniques were proposed. In [15] a sensor-less technique is proposed. Also, in several studies Space Vector Modulation (SVM) [16] is used to generate continuous voltage vectors that can correctly and moderately modify torque and flux. However, rotary co-ordinate transformation is required in SVM-based DTC schemes, which is more computationally complex than standard DTC.

Another process to reduce torque ripple in DTC is using multi-level inverter [17]. An asymmetric cascaded multilayer inverter generates the voltage vector without the requirement for modulation or filtering. Here the torque ripple is minimized due to higher output quality of the inverter but. Cost of hardware is very much high for this process.[18].

Another method is duty cycle control, which is used in traditional DTC in order to reduce the torque ripple. In traditional DTC a voltage vector is applied for the whole period of time which results the torque and flux value to increase over the reference value and which ultimately causes torque ripple. Each sample period in this approach uses both an active vector and a zero vector. Duty cycle control was first proposed by Pengcheng Zhu, Yong Kang and Jian Chen in 2003 [19]. First it was implemented in Induction motor. Prime task for this method is to determine the duty ratio. Later D. -H. Lee, Y. -J. An and E. -C. Nho proposed a method for determining the duty ratio for PMSM drive [20]. In this method duty ratio is determined by the torque error and torque bandwidth. But the major drawback of this method is the torque ripple is dependent on hysteresis band. With the increase and decrease of hysteresis band the

torque ripple is also increased or decreased. In order to make it independent from torque hysteresis band a new method was proposed by I. R. Akhil and C. K. Vijayakumari [34]. Here the duty ratio is established only on the basis of torque error. So, here the ripple content can be reduced independent of the bandwidth of torque hysteresis controller.

Using the MTPA equation from [22], a relationship between torque and flux has been developed in this article. The torque is then determined by converting the estimated flux using that equation. After that comparing with reference torque, the torque error has been generated and the duty ratio have been calculated using that torque error. Now on time  $t_k$  for duty ratio control is calculated by taking average of on times of conventional DTC and MTPA based DTC. This method gives a considerable reduction in torque ripple.

All of the simulations are carried out in MATLAB Simulink and contrasted with alternative approaches using identical conditions. Here are the data, which demonstrate a notable decrease in torque ripple.

## **1.4 Organization of Thesis**

The thesis is structured as follows:

- **Chapter 1** Contains the basic idea behind the thesis work. A brief history of permanent magnet machines, my inspiration for this work, a study of the literature on the subject, as well as a discussion of its limitations, are all included.
- **Chapter 2** contains detailed information about PMSM. Stator and rotor construction, working principle and complete mathematical model of PMSM is discussed here.
- **Chapter 3** consists of detailed information regarding voltage source inverter. Also, the power devices used in voltage source inverter, VSI topology and the switching states of the inverter is discussed here.

- In **chapter 4** In-depth discussion is given on direct torque control. Following a brief introduction to DTC, the fundamentals of DTC and control topology are covered in this article. Following that, a schematic diagram for traditional DTC is displayed and discussed.
- **Chapter 5** addresses the use of duty ratio modulation. The purpose of employing this strategy and its use are then explored. Then, this section also describes the process for computing the duty ratio. Finally, here is a schematic diagram employing this methodology that is presented and discussed.
- In **chapter 6** maximum torque per ampere control is discussed here basis principal for MTPA is discussed. Then a relationship between torque and flux is established using MTPA.
- **Chapter 7** contains the proposed method which is used in this work. Also, a schematic diagram of proposed method is shown and discussed here.
- **Chapter 8** is the most important chapter where responses the responses obtained from MATLAB for all the important parameters for all cases has been shown. Then the responses are compared with each other and the ripple percentages, observations from the results are discussed.
- **Chapter 9** is the thesis's conclusion. Here, I outline my contributions to the project and any potential future implications of my work.

# Chapter 2

## Permanent Magnet Synchronous Motor

### **2.1** Introduction

The Permanent Magnet Synchronous Motor (PMSM) is a type of Synchronous motor in which permanent magnets are used to energise the rotor field. It is brushless with very high reliability and efficiency. Permanent magnets are utilised to produce a spinning magnetic field rather than winding for the rotor. This kind of motor does not need a DC source to power the rotor. Because there is no DC supply, these motors are simple and inexpensive. As a general principle, it is an AC-synchronous motor with a sinusoidal back EMF waveform that is powered by permanent magnets. In order to create torque at zero speed, the PMSM relies on the permanent magnets. A digitally controlled inverter is required for this motor to perform at its peak efficiency [23] [2].

### **2.2** Construction Of PMSM

The stator and rotor are the two primary components of PMSM. The armature winding of the motor is done by the stator, which is the part that doesn't move. The field winding is done by the rotor. The armature winding is the main winding because it induces EMF in the motor. The field winding is carried by the rotor the main field flux is induced in the rotor through permanent magnets. Material with excellent permeability and coercivity is used in the construction of these Permanent Magnets These materials are Samarium-Cobalt and Neodimium-Iron-Boron.[2][25].

#### **2.2.1 Rotor Construction:**

As discussed earlier the rotor of PMSM is made of permanent magnet and rare earth material with high coercive force is used as permanent magnets. According to the shape design of the rotor the rotors are specified into two types [26]:

## 1. Salient pole rotor

## 2. non-salient pole rotor.

The non-salient pole rotors are cylindrical in shape. For this type of rotor there is a uniform air gap between stator and rotor. Due to this uniform air gap the direct and quadrature axis inductances of this type of rotor are equal  $L_d = L_q$  [26].

The Salient pole type rotors do not have a uniform air gap between stator and rotor. So, for this kind of rotor the direct and quadrature axis inductances are not equal  $L_d \neq L_q$  [26].

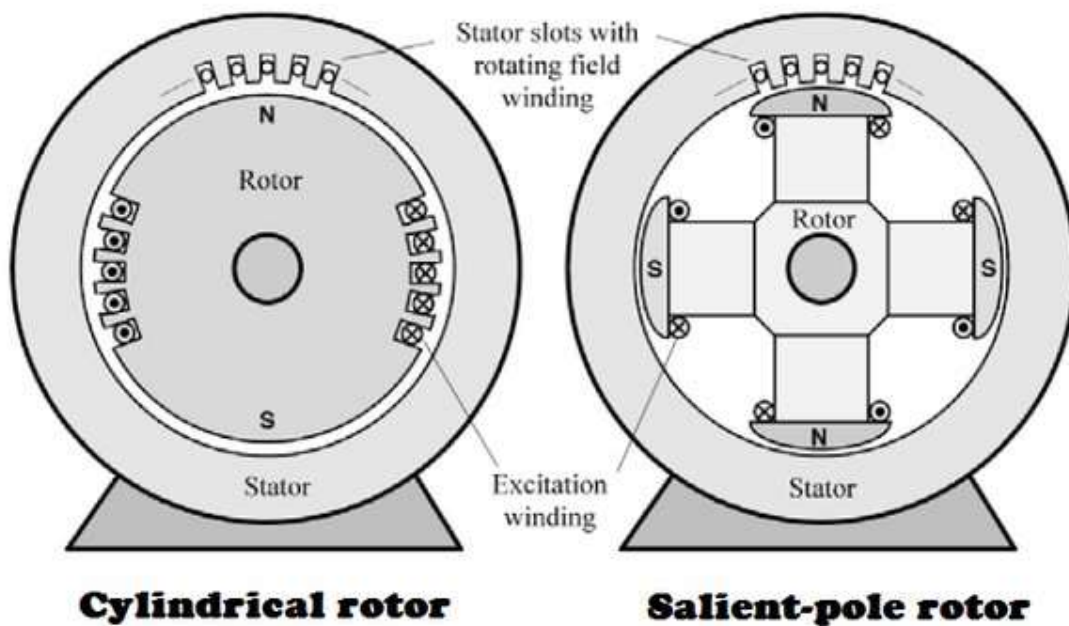


Fig 2.1 : Comparison between cylindrical rotor and Salient pole Synchronous machine

According to the arrangement of the permanent magnet in the rotor there several type of rotor. Here, we talk about some of the most common arrangements and how they affect the airgap flux density, winding inductances, and reluctance torque.

**1. Surface-Mounted PMSM:** In this type of set-up, the magnets are attached to the surface of the rotor laminations on the outer edge. This kind of arrangement doesn't get interrupted by anything else, like rotor lamination. It has the maximum air gap flux density because it confronts the air gap directly. However, this kind of design has several drawbacks. This kind of configuration has a poor level of structural integrity and mechanical toughness. In practical PMs are buried into the rotor laminations using Kavalier tape. So that it can provide some mechanical strength. Also, the magnets are bound to the rotor. So, it reinforces the mechanical strength of the rotor. These arrangements are not preferred for high-speed applications. The difference in reluctance between the direct and quadrature axes in this machine is very small because it is built like a non-salient pole. The variation between the quadrature and direct axes inductances is less than 10% [3] [24].

**2. Surface-Inset PMSM:** In this kind of set-up, the magnets are put in the grooves around the outside of the rotor laminations. Because of this, it gives the rotor a smooth, round surface. This set-up is much more mechanically stable than the last one. The magnets are fully and mechanically embedded in the rotor which gives it mechanical strength from flying out. In this machine, the difference between the inductances of the quadrature and direct axes can be as high as 2-2.5 [3] [24].

**3. Interior PMSM:** In this type of setup, the magnets are placed in the middle of the rotor laminations in either a radial or circumferential direction. This design is strong in terms of mechanics, so it can be used for high-speed applications. This set-up is harder to make than magnet rotors that are surface mounted or set inside a housing. Note that the ratio between the inductances of the quadrature and direct axes is between 3 and 1. But there have been claims that other interior PM rotor configurations have a much higher ratio [24].

In this kind of set-up, sometimes some steel is taken out of the rotor to make big air gaps between the magnets in the rotor. This is done to stop flux from moving from one PM to the next on the upper rotor surface. The flux will move from one magnet to the next one in the rotor, bypassing the structure of the stator. This means that there



will be less mutual flux linkages. The weight of the rotor also becomes less which gives lowest rotor inertia. So, it provides higher acceleration rates.

Another type of inset rotor is the circumferential inset PM rotor. It requires a large volume of the PMs. So, this setup can only be used with low-cost, low-energy magnets like ferrites, since high-energy magnets are expensive. In this setup, the air gap flux density can be made higher because the cross-sectional area of the magnets is much bigger than the surface area of the rotor that carries the flux from a magnet to the stator. Because of the higher air gap flux density, this setup is very desirable from the viewpoint of better efficiency and relatively small stator excitation for same power output [3] [24].

### **2.2.2 Stator Construction:**

The stator is constructed with two parts at the out most surface there is an outer frame. This has a core with windings inside of it. Windings with two or three phases are the most prevalent.

The two kinds of permanent magnet synchronous motors are distinguished by the stator design:

1. PMSM with a distributed winding
2. PMSM with a concentrated winding [26].

**1. Distributed winding:** In this type of windings the number of slots per pole and phase  $Q = 2, 3, \dots, k$ .

**2. Concentrated winding:** The number of slots per pole and phase  $Q = 1$  in this type of winding. The slots on this stator are uniformly spaced all the way around its circumference. These windings are made up of two coils that can be linked either in parallel or in series. The main problem with these windings is that you can't change the shape of the EMF curve [25][26].

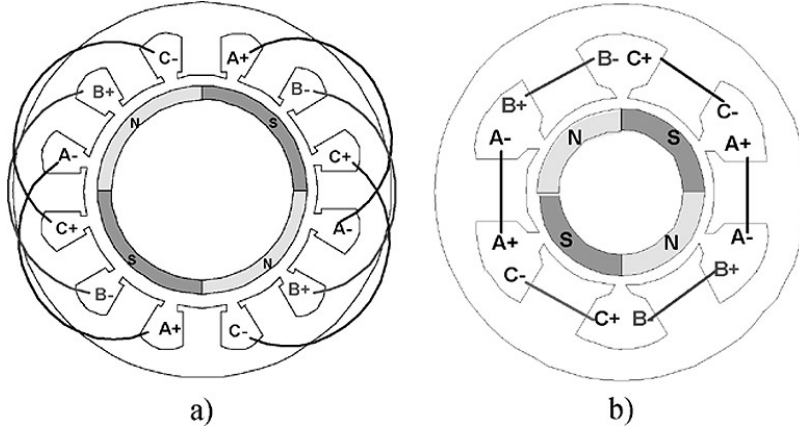


Fig 2.2 (a) Distributed windings. (b) Concentrated windings.

## **2.3 Working Principle of PMSM**

The Working Principle of PMSM is based on the interaction of the rotating magnetic field generated through 3 phase ac supply in stator and the constant magnetic field of the rotor generated via permanent magnet.

The rotating magnetic field in air gap via stator is generated in the same way like in a 3-phase induction motor. The generated rotating magnetic field revolve in synchronous speed and it can be calculated by,  $N_s = 120 * f / P$  this equation here  $f$  denotes frequency of supply and  $P$  denotes number of poles.

By joining the windings of the stator with one another phasor groups are created and by joining theses phasor groups to gather different connections like a star, Delta, double and single phases are formed. The windings are wound shortly with each other to reduce harmonic voltages.

The permanent magnets used as the rotor creates constant magnetic flux. When the constant magnetic field of rotor locks with the rotating magnetic field in the air gap generated by stator the rotor starts to rotate in synchronous speed. The rotor rotates in synchronous speed regardless of the applied load torque. When the applied load torque crosses the maximum limit, the rotor become standstill [2][25][26].

## 2.4 Mathematical Modelling of PMSM

Here, Complete mathematical model of the motor is derived for proper simulation and analysis of the system. For ease of calculation the motor axis has been developed using d-q rotor reference frame theory [1]. The rotor reference frame makes an angle  $\theta_r$  with the fixed stator axis at any time instance t. The stator MMF makes an angle  $\alpha$  with the rotor d-axis, and at any time t, the stator MMF spins at the very same speed as the rotor axis [3].

There are some assumptions made in the process:

- 1) Eddy current and hysteresis losses are insignificant.
- 2) The Induced EMF is sinusoidal in nature;
- 3) Saturation isn't taken into account, but parameter changes can do that;
- 4) No field current dynamics.

### 2.4.1 Three phase to two phase transformations (ABC to DQ):

It can be done by changing the voltages and currents of the three phases ABC to  $\alpha\beta$  axis variables by using the Clarke transformation.  $f_{\alpha\beta} = K_1 \cdot f_{abc}$ . After that to transform it from  $\alpha\beta$  to d-q Clarke transformation is used.  $f_{qd} = K_2 \cdot f_{\alpha\beta} = K_2 \cdot K_1 \cdot f_{abc} = K \cdot f_{abc}$ . D-Q Modeling of the system is used to study the motor in both the steady state and the transient state [28].

$$K_1 = \frac{2}{3} \cdot \begin{bmatrix} 1 & -\frac{1}{2} & -\frac{1}{2} \\ 0 & \frac{\sqrt{3}}{2} & -\frac{\sqrt{3}}{2} \\ \frac{1}{2} & \frac{1}{2} & \frac{1}{2} \end{bmatrix} \dots (2.1) \text{ and, } K_2 = \begin{bmatrix} \cos \theta & -\sin \theta & 0 \\ \sin \theta & \cos \theta & 0 \end{bmatrix} \dots (2.2)$$

Hence,  $K$  can be calculated as,

$$K = \frac{2}{3} \cdot \begin{bmatrix} \cos(\theta) & \cos(\theta - \frac{2\pi}{3}) & \cos(\theta + \frac{2\pi}{3}) \\ \sin(\theta) & \sin(\theta - \frac{2\pi}{3}) & \sin(\theta + \frac{2\pi}{3}) \end{bmatrix}, \dots (2.3)$$

$$\text{Consequently, } K^{-1} = \begin{bmatrix} \cos(\theta) & \sin(\theta) \\ \cos(\theta - \frac{2\pi}{3}) & \sin(\theta - \frac{2\pi}{3}) \\ \cos(\theta + \frac{2\pi}{3}) & \sin(\theta + \frac{2\pi}{3}) \end{bmatrix} \dots (2.4)$$

Three phase voltages ( $v_a, v_b, v_c$ ) of the inverter are converted to  $D - Q$  axis voltages ( $v_d, v_q$ ) by using Park transformation shown below [3][1]:

$$\begin{bmatrix} v_q \\ v_d \\ v_0 \end{bmatrix} = \frac{2}{3} \begin{bmatrix} \cos(\theta) & \cos(\theta - \frac{2\pi}{3}) & \cos(\theta + \frac{2\pi}{3}) \\ \sin(\theta) & \sin(\theta - \frac{2\pi}{3}) & \sin(\theta + \frac{2\pi}{3}) \end{bmatrix} \begin{bmatrix} v_a \\ v_b \\ v_c \end{bmatrix}$$

The inverse Park transform, as stated below, is used to derive  $abc$  variables from  $d, q$  variables [3].

$$\begin{bmatrix} v_a \\ v_b \\ v_c \end{bmatrix} = \begin{bmatrix} \cos(\theta) & \sin(\theta) \\ \cos(\theta - \frac{2\pi}{3}) & \sin(\theta - \frac{2\pi}{3}) \\ \cos(\theta + \frac{2\pi}{3}) & \sin(\theta + \frac{2\pi}{3}) \end{bmatrix} \begin{bmatrix} v_q \\ v_d \\ v_0 \end{bmatrix}$$

### 2.4.2 Motor modelling:

The equivalent circuit model based on d- and q-coordinates is used to model PMSMs. A conceptual cross-sectional image of a 3-phase, 2-pole interior PMSM is shown in Fig. 2.4, along with two reference frames. We assume that the permanent magnet rotor generates magnetic flux in the direction of the d-axis  $\Psi_r$ .

Along the a-phase, b-phase, and c-phase axes of the stator, the components of this rotor flux are,  $\Psi_r \cos(\theta), \Psi_r \cos(\theta - \frac{2\pi}{3})$  and  $\Psi_r \cos(\theta + \frac{2\pi}{3})$  respectively. Thus, phase flux linkages can be expressed as [3]:

$$\Psi_a = L_{aa} \cdot i_a + L_{ab} \cdot i_b + L_{ac} \cdot i_c + \Psi_r \cdot \cos(\theta) \quad \dots (2.5)$$

$$\Psi_b = L_{ba} \cdot i_a + L_{bb} \cdot i_b + L_{bc} \cdot i_c + \Psi_r \cdot \cos(\theta - \frac{2\pi}{3}) \quad \dots (2.6)$$

$$\Psi_c = L_{ca} \cdot i_a + L_{cb} \cdot i_b + L_{cc} \cdot i_c + \Psi_r \cdot \cos(\theta + \frac{2\pi}{3}) \quad \dots (2.7)$$

Here,  $L_{kk}$  is the self-inductance of the  $k$ -th phase and  $L_{ij}$  is the mutual inductance of  $i$ -th phase due to  $j$ -th phase.

Due to the balanced mode of PMSM with symmetrical alignments of the inductances, we can consider,

$$L_{kk} = L \text{ for } k = a, b \text{ or } c$$

$$L_{ij} = L_m \text{ for all } i \text{ and } j.$$

So, in balanced condition, the sum of the stator currents equal to zero, i.e.  $i_a + i_b + i_c = 0$ ,

Due to these the simplified phase flux linkage equations provide the following results:

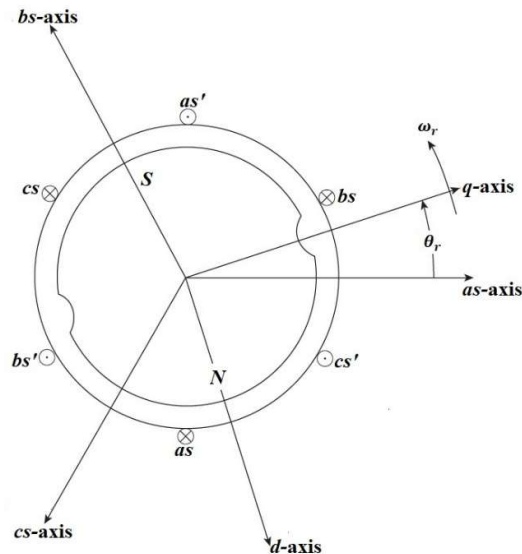


Fig 2.3 Motor Axis Diagram

$$\Psi_a = (L - L_m) \cdot i_a + \Psi_r \cdot \cos(\theta) \quad \dots (2.8)$$

$$\Psi_b = (L - L_m) \cdot i_b + \Psi_r \cdot \cos\left(\theta - \frac{2\pi}{3}\right) \quad \dots (2.9)$$

$$\Psi_c = (L - L_m) \cdot i_c + \Psi_r \cdot \cos\left(\theta + \frac{2\pi}{3}\right) \quad \dots (2.10)$$

The stator phase voltages in balanced mode may now be expressed as,

$$v_a = R_s \cdot i_a + \frac{d\Psi_a}{dt} \quad \dots (2.11)$$

$$v_b = R_s \cdot i_b + \frac{d\Psi_b}{dt} \quad \dots (2.12)$$

$$v_c = R_s \cdot i_c + \frac{d\Psi_c}{dt} \quad \dots (2.13)$$

If we consider,  $[f_{abc}] = [f_a \ f_b \ f_c]^T$ , then the above set of equations can be written as,

$$[v_{abc}] = R_s \cdot I_{3 \times 3} \cdot [i_{abc}] + \frac{d}{dt} [\Psi_{abc}] \quad \dots (2.14)$$

and essentially the expression of  $[\Psi_{abc}]$  is as,

$$[\Psi_{abc}] = (L - L_m) \cdot I_{3 \times 3} \cdot [i_{abc}] + \Psi_r \cdot [A_{cos}] \quad \dots (2.15)$$

where we have,  $[A_{cos}] = \begin{bmatrix} \cos(\theta) \\ \cos\left(\theta - \frac{2\pi}{3}\right) \\ \cos\left(\theta + \frac{2\pi}{3}\right) \end{bmatrix}$

Now the transformation of  $[\Psi_{abc}]$  to  $[\Psi_{dq}]$  reference frame is done,

$$[\Psi_{dq}] = (L - L_m) \cdot I_{2 \times 2} \cdot [i_{dq}] + \Psi_r \cdot \begin{bmatrix} 0 \\ 1 \end{bmatrix} \quad \dots (2.16)$$

And, to frame  $[v_{dq}]$  can be written as,

$$[v_{dq}] = R_s \cdot I_{2 \times 2} \cdot [i_{dq}] + K \cdot \frac{d}{dt} K^{-1} [\Psi_{dq}] \dots (2.17)$$

Following fundamental calculus on matrix- expressions we get,

$$\frac{d}{dt} K^{-1} [\Psi_{dq}] = \left[ \frac{d}{dt} K^{-1} \right] \cdot [\Psi_{dq}] + K^{-1} \cdot \frac{d}{dt} [\Psi_{dq}]$$

Hence,  $K \cdot \frac{d}{dt} K^{-1} [\Psi_{dq}]$  is expressed as,

$$K \cdot \frac{d}{dt} K^{-1} [\Psi_{dq}] = K \cdot \left[ \frac{d}{dt} K^{-1} \right] \cdot [\Psi_{dq}] + \frac{d}{dt} [\Psi_{dq}]$$

Following simple calculations we have,

$$K \cdot \left[ \frac{d}{dt} K^{-1} \right] = \begin{bmatrix} 0 & -1 \\ 1 & 0 \end{bmatrix} \cdot \frac{d\theta}{dt} = \begin{bmatrix} 0 & -1 \\ 1 & 0 \end{bmatrix} \cdot \omega_s$$

Following fundamental calculus on matrix- expressions we get,

$$\frac{d}{dt} K^{-1} [\Psi_{dq}] = \left[ \frac{d}{dt} K^{-1} \right] \cdot [\Psi_{dq}] + K^{-1} \cdot \frac{d}{dt} [\Psi_{dq}]$$

Hence,  $K \cdot \frac{d}{dt} K^{-1} [\Psi_{dq}]$  is expressed as,

$$K \cdot \frac{d}{dt} K^{-1} [\Psi_{dq}] = K \cdot \left[ \frac{d}{dt} K^{-1} \right] \cdot [\Psi_{dq}] + \frac{d}{dt} [\Psi_{dq}]$$

Following simple calculations we have,

$$K \cdot \left[ \frac{d}{dt} K^{-1} \right] = \begin{bmatrix} 0 & -1 \\ 1 & 0 \end{bmatrix} \cdot \frac{d\theta}{dt} = \begin{bmatrix} 0 & -1 \\ 1 & 0 \end{bmatrix} \cdot \omega_s$$

Finally, the expression of  $[v_{dq}]$  becomes,

$$[v_{dq}] = I_{2 \times 2} \cdot [i_{dq}] + (L - L_m) \cdot I_{2 \times 2} \cdot \frac{d}{dt} [i_{dq}] + \begin{bmatrix} 0 & -1 \\ 1 & 0 \end{bmatrix} \cdot \omega_s \cdot [\Psi_{dq}] \dots (2.18)$$

$$[\Psi_{dq}] = (L - L_m) \cdot I_{2 \times 2} \cdot [i_{dq}] + \Psi_r \cdot \begin{bmatrix} 0 \\ 1 \end{bmatrix}, \dots (2.19)$$

this implies,

$$\begin{bmatrix} 0 & -1 \\ 1 & 0 \end{bmatrix} \cdot \omega_s \cdot [\Psi_{dq}] = \begin{bmatrix} -(L - L_m) \cdot \omega_s \cdot i_q \\ (L - L_m) \cdot \omega_s \cdot i_d + \omega_s \cdot \Psi_r \end{bmatrix} \dots (2.20)$$

And finally substituting this in the expression of  $[v_{dq}]$  we get,

$$v_d = R_s \cdot i_d - (L - L_m) \cdot \omega_s \cdot i_q + (L - M) \cdot \frac{di_d}{dt} \dots (2.21)$$

$$v_q = R_s \cdot i_q + (L - L_m) \cdot \omega_s \cdot i_d + (L - M) \cdot \frac{di_q}{dt} + \omega_s \cdot \Psi_r \dots (2.22)$$

We are considering the balanced mode, and so we may consider,  $(L - L_m) = L_d = L_q$  and this reveals the expression of  $v_d$  and  $v_q$  as,

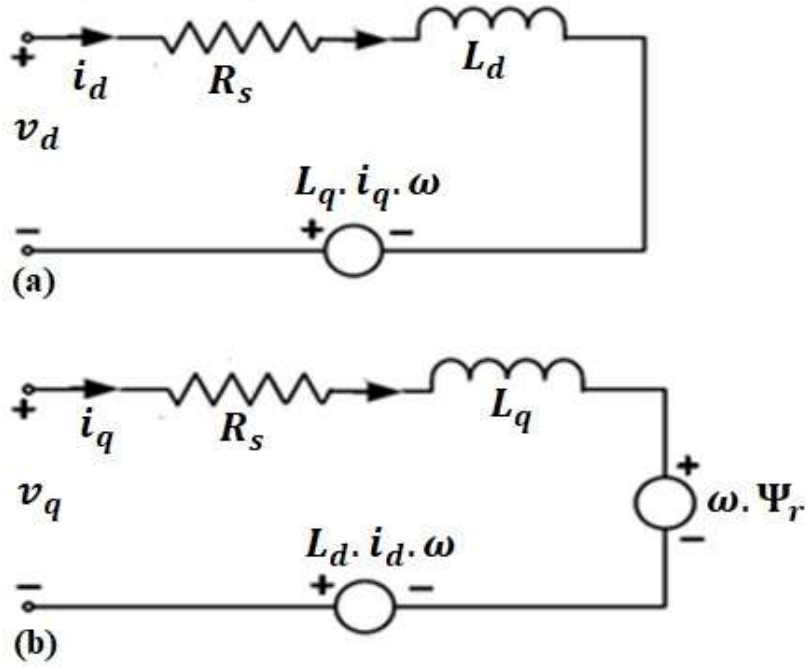
$$v_d = R_s \cdot i_d - L_q \cdot i_q \cdot \omega_s + L_d \cdot \frac{di_d}{dt} \dots (2.23)$$

$$v_q = R_s \cdot i_q + L_d \cdot i_d \cdot \omega_s + L_q \cdot \frac{di_q}{dt} + \omega_s \cdot \Psi_r \dots (2.24)$$

To define the flux linkage of the transformed axes, we follow,

$$\begin{bmatrix} 0 & -1 \\ 1 & 0 \end{bmatrix} \cdot \omega_s \cdot [\Psi_{dq}] = \begin{bmatrix} -(L - L_m) \cdot \omega_s \cdot i_q \\ (L - L_m) \cdot \omega_s \cdot i_d + \omega_s \cdot \Psi_r \end{bmatrix}$$





Which implies,  $[\psi_{qd}] = \begin{bmatrix} \psi_q \\ \psi_d \end{bmatrix} = \begin{bmatrix} L_q \cdot i_q \\ L_d \cdot i_d + \psi_r \end{bmatrix} \dots (2.25)$

Therefore, following equation (3) the dynamic equivalent circuit of PMSM in d-q frame can be depicted as,

### 2.4.3 Electromagnetic Torque Equation:

We ignore the magnetic field saturation situation, as well as losses owing to eddy currents and hysteresis, in order to suggest power invariant transformation. And we obtain,

$$P_{in} = P_{out} = \frac{3}{2} (v_q \cdot i_q + v_d \cdot i_d) \dots (2.26)$$

Substituting the values of  $v_q$  and  $v_d$  we get,

Fig:2.4 (a) D-axis circuit and (b) Q-axis circuit

$$P_{out} = \frac{3}{2} (\Psi_d \cdot i_q - \Psi_q \cdot i_d) \cdot \omega_s \quad \dots (2.27)$$

Therefore, the total electrical torque is expressed as,

$$T_e = (Pole\ Pair) \cdot \frac{P_{out}}{\omega_s} = P \cdot \frac{3}{2} \cdot (\Psi_d \cdot i_q - \Psi_q \cdot i_d) \quad \dots (2.28)$$

Substituting the values of  $\phi_d$  and  $\phi_q$  we get,

$$T_e = P \cdot \frac{3}{2} \cdot (\{L_d - L_q\} \cdot i_d \cdot i_q + \Psi_r \cdot i_q) \quad \dots (2.29)$$

#### 2.4.4 Mechanical system model:

The system's load torque, accelerating torque, and damping torque balance the electromagnetic torque, which may be expressed as [22] [27]:

$$T_e = T_L + B \cdot \omega_r + J \cdot \frac{d}{dt} \omega_r \quad \dots (2.30)$$

Where,  $T_L$  is the load torque,  $B$  is the damping coefficient and  $J$  is the moment of inertia.

$$\omega_s = (Pole\ Pair) \cdot \omega_r$$

#### 2.4.5 Final modelling equation:

For the purpose of dynamic simulation, the equations can be re arranged to give first order nonlinear differential equations in terms of variables as [22],[27]:

$$\frac{d}{dt} i_d = (v_d - R_s \cdot i_d + \omega_s \cdot L_q \cdot i_q) / L_d \quad \dots (2.31)$$

$$\frac{d}{dt} i_q = (v_q - R_s \cdot i_q - \omega_s \cdot L_d \cdot i_d - \omega_s \Psi_r) / L_q \quad \dots (2.32)$$

$$\frac{d}{dt} \omega_r = \frac{(T_e - T_L - B \cdot \omega_r)}{J} \quad \dots (2.33)$$

$$\omega_r = \int \frac{(T_e - T_L - B \cdot \omega_r)}{J} \quad \dots (2.34)$$

$$\frac{d}{dt} \theta = \omega_r \quad \dots (2.35)$$

Combining the set of equations, we can develop a complete states space dynamic model of PMSM in d-q reference frame.

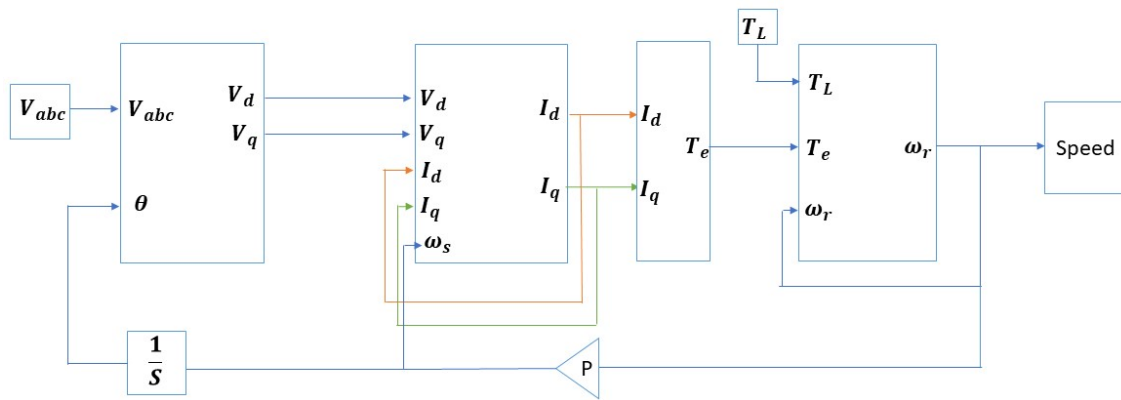


**Fig 2.5 Simulink Based Model of PMSM**

# Chapter 3

## Voltage Source Inverter

### **3.1** Introduction

The standard power electronic inverter modules are the subsystem that allowed the widespread usage of permanent magnet (PM) drives practicable. Inversion is the process of converting dc to alternating current power, and it is the inverter that generates the variable frequency from the dc source that is utilized to drive a permanent magnet synchronous motor at a variable speed [3].

For the process of DTC, a three-phase voltage source inverter with 180-degree conduction mode is used here.

### **3.2** Power devices used in VSI

Voltage, current, power, and frequency control have all become more affordable since the invention of semiconductor power switches. Some power electronic devices those are used as active switches in VSI are:

- Diode
- Thyristor or silicon-controlled rectifier (SCR)
- Gate Turn off Thyristor (GTO)
- Bipolar junction transistor (BJT)
- Power MOSFET
- Insulated Gate Bipolar Junction Transistor (IGBT)

These power electronic devices are generally used as switch of VSI.

### **3.3** VSI Topology

The usage of three-phase bridge inverters for general-purpose ac supply and ac motor drives is very common. The voltage source inverter (VSI) is generally utilized in the

DTC. VSI may be two-level or multi-level inverter, but this work will concern on the two-level type as it is the most common type. In figure 3.1 the basic topology of the inverter is shown. Figure 3.2 Explains how square wave, or six-step, mode of operation generates the output voltage waves. To create the three-phase voltage waves, the circuit consists of three half-bridges that are phase-shifted by an angle of  $2\pi/3$  [30].

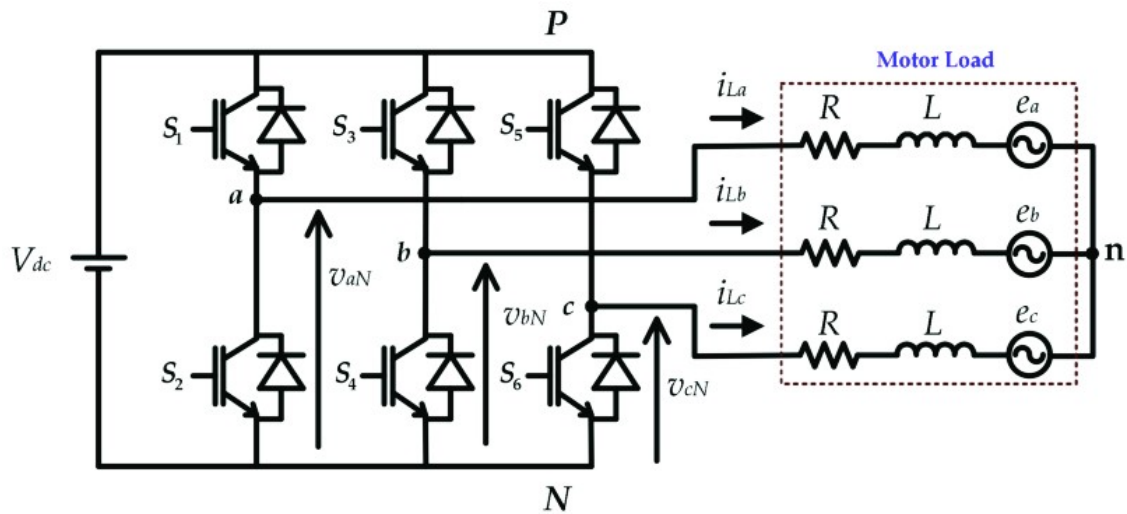


Figure 3.1 Topology of Voltage source inverter

The six switches are divided into two groups. The top three switches (S1, S3, and S5) make up the positive group, and the bottom three switches make up the negative group (i.e., S4, S6, S2). Six of the eight possible switching states (1–6) are active and produce non-zero ac output voltages. The other two states have no voltage (0 and 7) [30].

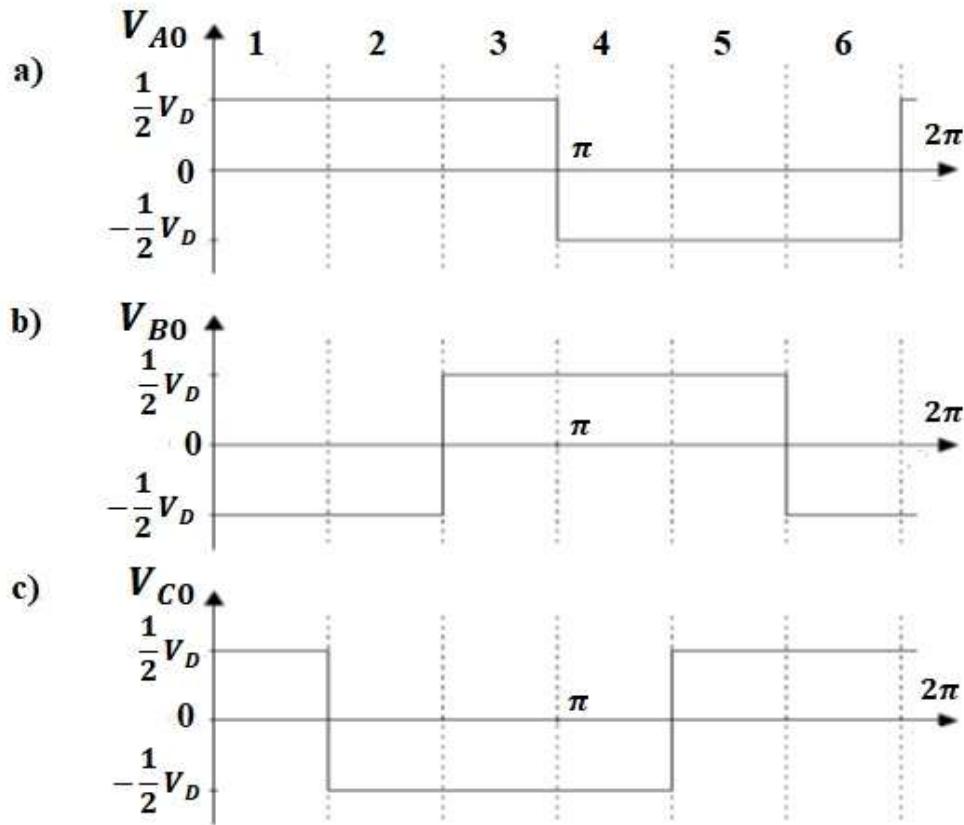


Figure 3.2 Phase voltages for 180-degree conduction mode

State	$S_A$	$S_B$	$S_C$	Vector
0	0	0	0	$V_0$
1	1	0	0	$V_1$
2	1	1	0	$V_2$
3	0	1	0	$V_3$
4	0	1	1	$V_4$
5	0	0	1	$V_5$
6	1	0	1	$V_6$
7	1	1	1	$V_7$

**Table 3.1 Switching state of 3-phase Voltage source inverter**

### 3.4 Switching States of VSI

The three phase stator voltages of the motor  $V_A$ ,  $V_B$  and  $V_C$  are decided by the states of the 3 switches  $S_A$ ,  $S_B$  and  $S_C$ . If  $S_A$  is 1 that means  $V_A$  is connected to +ve terminal of DC supply and if  $S_A$  is 0 that means  $V_A$  is connected to -ve terminal of DC supply. The same cases are for  $V_B$  and  $V_C$ . For example, if  $(S_A, S_B, S_C) = (1,0,0)$  then  $V_A$  is connected to the +ve terminal of the battery and both of  $V_B$  and  $V_C$  are connected to the -ve terminal. The resultant voltage vector ( $V_1$ ) can be calculated as [29]:

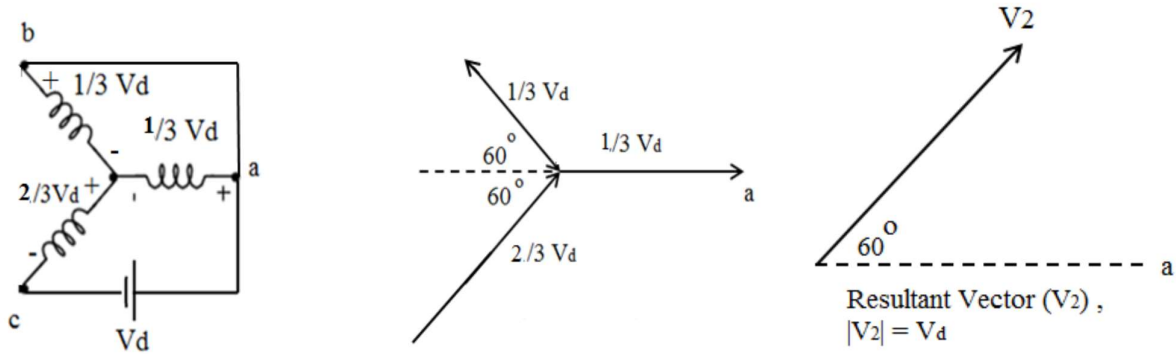


Figure 3.3 The Resultant Voltage Vector of the Switching Status (1, 0, 0)

$$V_1 = \frac{2}{3} V_D + \frac{1}{3} V_D \cdot \cos 60 + \frac{1}{3} V_D \cdot \cos 60 = V_D \quad \dots (3.1)$$

For the switching status (1, 1, 0), both of  $V_A$  and  $V_B$  are connected to the +ve terminal of  $V_D$  and  $V_C$  is connected to the -ve terminal. The resultant voltage vector has a magnitude of  $V_d$  and  $60^\circ$  apart from the reference (phase a). The resultant voltage vector ( $V_2$ ) can be calculated as [29]:

$$V_2 = \frac{2}{3} V_D \angle 60^\circ + \frac{1}{3} V_D + \frac{1}{3} V_D \angle 120^\circ = V_D \angle 60^\circ \quad \dots (3.2)$$



Therefore, there are eight voltage vectors, six are non-zero voltage vectors (active voltage vectors):  $V_1$  (100),  $V_2$  (110),  $V_3$  (010),  $V_4$ (011),  $V_5$  (001), and  $V_6$  (101) and two zero voltage vectors  $V_0$  (000) and  $V_7$  (111).

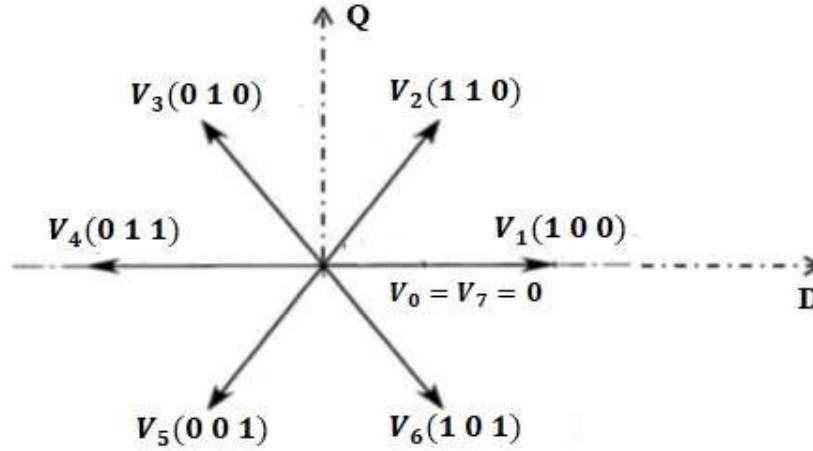


**Figure 3.4 Inverter Eight Voltage Vectors in D-Q plane**

A method known as space vector pulse width modulation can be used to combine the non-zero voltage vectors and the zero voltage vectors to produce additional voltage vectors that are different from these eight vectors (SV-PWM). The average of the needed voltage vector in SV-PWM should match the average of the voltage the inverter produces.

The needed voltage vector is created by applying two non-zero voltage vectors for times  $T_1$  and  $T_2$ , respectively, and a zero-voltage vector for time  $T_0$ , where the total of these times  $T_1$ ,  $T_2$ , and  $T_0$  equals the sampling time  $T_s$ . We may derive the times  $T_1$  and  $T_2$  by equating the "Volt. Sec." in both the D- and Q-planes.  $T_0$  is obtained by subtracting  $T_1$  and  $T_2$  from  $T_s$ .

# Chapter 4

## Traditional Direct Torque control (DTC)

### Method

#### 4.1 Introduction

Basic idea of conventional DTC is to select the stator voltage vectors directly based on differences between reference and actual torque and flux values. Without the need for coordinate transformation, torque and flux are immediately regulated and resolved using nonlinear transformations on hysteresis controllers. The motor, a three-phase voltage source inverter, and a speed controller to produce the torque command are included in this power supply circuit. The standard DTC system is a closed loop control scheme. [31].

The DTC controller is comprised of a sector selection block, stator flux estimate blocks, 2 different hysteresis controllers (Flux and torque). The DTC controller sends gating pulses to the inverter.

The DTC system does not need coordinate transformation, because all control actions are performed in a stationary frame of reference. As a result, this system is not as susceptible to parameter fluctuations as other control techniques. There is also no feedback current control loop, thus control operations are not delayed as they are with current controllers. Also, there is no PI controller, rotor speed or position sensor, or pulse width modulator. So, it is a sensor-less control system because it doesn't need a mechanical sensor on the shaft to run the motor. To close the loop, on-line torque and flux estimators are utilised. Here, hysteresis comparators are used to directly regulate the torque and stator flux [32].

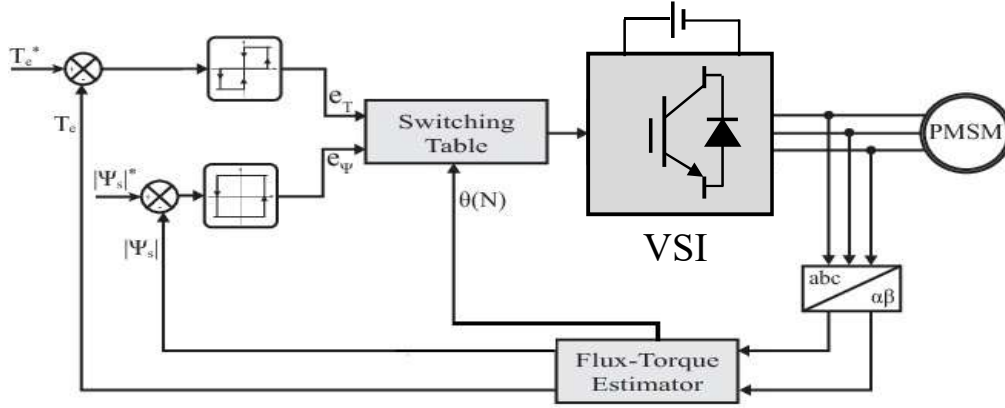


Figure 4.1 Schematic diagram of Conventional Direct Torque Control

The interaction of stator and rotor fields produces the governing equation for torque in this design. Torque and stator flux linkage are calculated using motor terminal data such as stator voltages and current. The hysteresis control of stator flux and torque selects an appropriate voltage vector for VSI switching from among six nonzero voltage vectors and two zero voltage vectors.

This control approach entails a comparative control of the torque and stator flux. It is more commonly used in regulating electrical machines since it is a simple and urable approach. Because the stator current and voltage are regulated indirectly, no current feedback loops are necessary. The block diagram of conventional DTC is given below

## 4.2 Working Principal of DTC

In PMSM stator flux can be calculated using the equation below :

$$\psi_s = \int (v_s - R_s \cdot i_s) dt \quad \dots (4.1)$$

Here  $v_s$  and  $i_s$  denotes stator voltage and current respectively and  $R$  denotes the resistance of the stator windings.

The stator flux may be characterised as the time integration of the stator voltage, ignoring the stator resistance voltage drop. As the motor is powered by a 3- Phase

voltage supply the motor flux will build up in the direction of the voltage vector. The stator voltage vector may be any of the six non-zero vectors in Fig 4.2 or zero at any time if the inverter is operated in a certain switching mode.

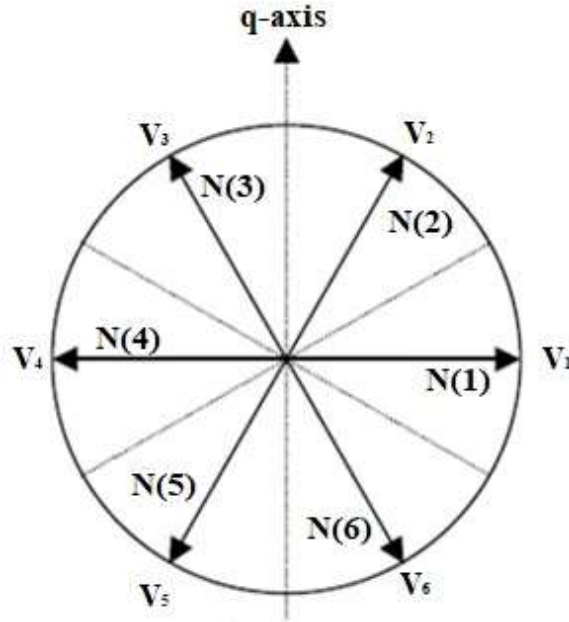


Figure 4.2 Voltage vectors and the six sectors for stator flux

So, in motoring mode an angle is created between the stator flux and rotor magnetic flux this angle is called load angle  $\delta$ .

Now if we divide the stator flux vector in d-q components we can write:

$$\psi_d^s = |\psi^s| \cos \delta \quad \dots (4.2)$$

$$\psi_q^s = |\psi^s| \sin \delta \quad \dots (4.3)$$

So, equation (2.16) can be re written as,

$$i_d = \frac{|\psi^s| \cos \delta - r}{L_d} \quad \dots (4.4)$$

$$i_q = \frac{|\psi^s| \sin \delta}{L_q} \quad \dots (4.5)$$

According to (2.29), (4.4), (4.5) we can say,

$$T_e = \frac{3}{2}P \left[ \psi_r \cdot \frac{|\psi^s| \sin \delta}{L_q} + (L_d - L_q) \cdot \frac{|\psi^s| \cos \delta - \psi_r}{L_d} \cdot \frac{|\psi^s| \sin \delta}{L_q} \right] \quad \dots (4.6)$$

Now, For an SPM (Surface Mounted Machine) with a consistent air gap  $L_q = L_d = L_s$ . So, equation (4.6) becomes

$$T_e = \frac{3}{2} \cdot \frac{P}{L_q} \cdot |\psi^s| \cdot \psi_r \cdot \sin \delta \quad \dots (4.7)$$

Torque increment equation can be written as

$$\Delta T_e = \frac{3}{2} \cdot \frac{P}{L_q} \cdot \psi_r |\psi^s| \Delta \delta \cdot \sin \Delta \delta \quad \dots (4.8)$$

From (4.7) and (4.8), we can see that the electromagnetic torque in a PMSM depends on the load angle ( $\delta$ ) and the strength of the stator flux ( $\psi^s$ ). As a result, stator flux

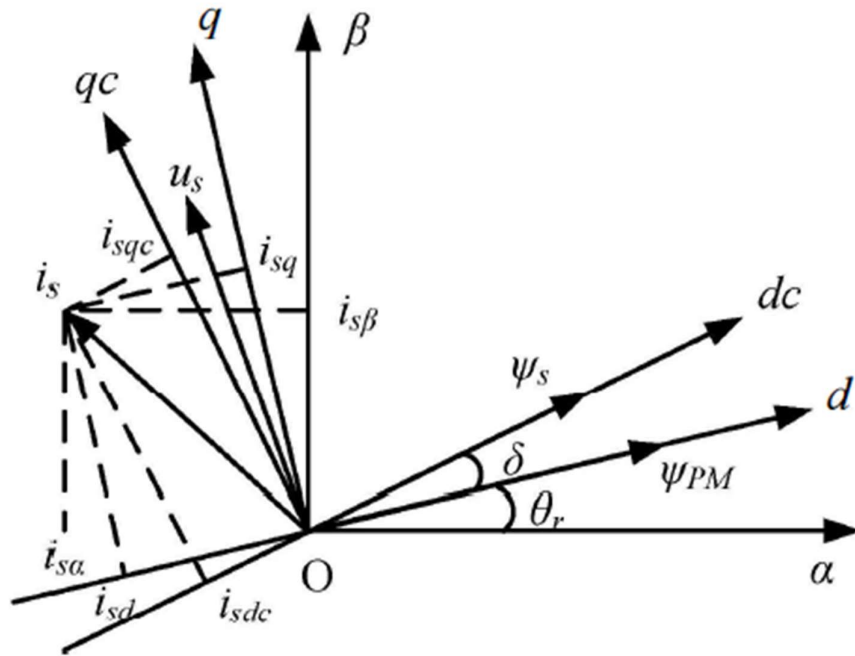


Figure 4.3 Stator and rotor flux in  $\alpha - \beta$  and d-q reference frame

may be used to adjust load angle as much as necessary to provide quick torque response. By selecting the proper switching of the inverter, we can adjust the stator flux a magnitude and the load angle [33]. In figure 4.3 a representation of stator and rotor flux in  $\alpha\beta$  and D-Q reference frame is shown.

### 4.3 Controller of DTC

A voltage vector is selected in DTC depending on the magnitude of the torque error, flux error, and the position of the sector in question. In this method, the active vector and the zero vector are employed at the same time in each sampling period.

#### 4.3.1 Flux and sector estimator

We require the coordinate transformation in this torque control system as the currents from the three-phase motor are sampled. Three phase voltages ( $v_a, v_b, v_c$ ) and currents ( $i_a, i_b, i_c$ ) of the inverter are converted to  $\alpha\beta$  axis voltages ( $v_\alpha, v_\beta$ ) and currents ( $i_\alpha, i_\beta$ ) by using Clarke transformation shown below. The relationship is demonstrated by the (4.9) and (4.10) functions.

$$\begin{bmatrix} i_\alpha \\ i_\beta \end{bmatrix} = \begin{bmatrix} 1 & -0.5 & -0.5 \\ 0 & \frac{\sqrt{3}}{2} & -\frac{\sqrt{3}}{2} \end{bmatrix} \begin{bmatrix} i_a \\ i_b \\ i_c \end{bmatrix} \quad \dots (4.9)$$

$$\begin{bmatrix} v_\alpha \\ v_\beta \end{bmatrix} = \begin{bmatrix} 1 & -0.5 & -0.5 \\ 0 & \frac{\sqrt{3}}{2} & -\frac{\sqrt{3}}{2} \end{bmatrix} \begin{bmatrix} v_a \\ v_b \\ v_c \end{bmatrix} \quad \dots (4.10)$$

A PMSM's stator flux linkage may be described in a stationary reference frame. According to Equation (2.11) :

$$v_s = R_s \cdot i_s + \frac{d\psi_s}{dt} \quad \dots (4.11)$$

$$\frac{d\psi_s}{dt} = v_s - R_s \cdot i_s \quad \dots (4.12)$$

$$\Psi_s = \int (v_s - R_s \cdot i_s) dt \quad .... (4.13)$$

It can be represented in  $\alpha$ - $\beta$  axis using following equations:

$$\psi_\alpha^s = \int (v_\alpha - R_s \cdot i_\alpha) dt \quad .... (4.14)$$

$$\psi_\beta^s = \int (v_\beta - R_s \cdot i_\beta) dt \quad .... (4.15)$$

Sector	Angle
1	<i>[-30, 30]</i>
2	<i>[30, 90]</i>
3	<i>[90, 150]</i>
4	<i>[150, 210]</i>
5	<i>[210, 270]</i>
6	<i>[270, 330]</i>

**Table 4.1 Sector selection table**

Now, the stator flux can be calculated using  $\psi_\alpha^s$  and  $\psi_\beta^s$ .

$$|\psi^s| = \sqrt{(\psi_\alpha^s)^2 + (\psi_\beta^s)^2} \quad .... (4.16)$$

The angle between two components of stator flux vector is defined using the following equation:

$$\alpha = \angle \psi^s = \tan^{-1} \left( \frac{\psi_{\beta}^s}{\psi_{\alpha}^s} \right) \quad \dots (4.17)$$

According to the angle  $\alpha$  the sector of the flux vector is estimated using the following table

### 4.3.2 Torque Estimation:

According to equation (2.28) the Electromagnetic torque can be estimated in  $\alpha\beta$  axis.

$$T_e = \frac{3}{2} \cdot P \cdot (\psi_{\alpha}^s \cdot i_{\beta} - \psi_{\beta}^s \cdot i_{\alpha}) \quad \dots (4.18)$$

### 4.3.3 Torque and Flux hysteresis controller

Two hysteresis controllers are required for DTC of an PMS motor. PMSM drive performance gets affected by the ripple in torque and flux, the current harmonics, and the switching speed of power electronics devices. Torque hysteresis bands minimize torque ripple, whereas flux hysteresis bands reduce current distortion. Every sampling time, the inverter's switching status is updated. The inverter state remains fixed until the hysteresis controller output states change within a sampling interval. If the hysteresis band remains constant, the switching frequency is entirely determined by the rate of change of torque and flux.

#### 4.3.3.1 Flux Hysteresis Controller

By comparing the flux reference point with the estimated flux ( $\psi_{ref} - \psi^s = \psi_{err}$ ) the flux error is calculated. If this error exceeds the hysteresis band limit, the flux controller output is high "1." If the mistake is inside the hysteresis range, the output is a low "0," as shown in Figure (4.4). If the output is high, it indicates that a flux increase is necessary, whereas a low output indicates that a flux drop is required. The flux controller's bandwidth is  $2H_{\psi}$  [21].



The output signal of hysteresis flux controller is defined as given below:

$$d\psi_s = \begin{cases} 1, & \psi_s < \psi_{ref} - H_\psi \\ 0, & \psi_s < \psi_{ref} + H_\psi \end{cases} \dots (4.20)$$

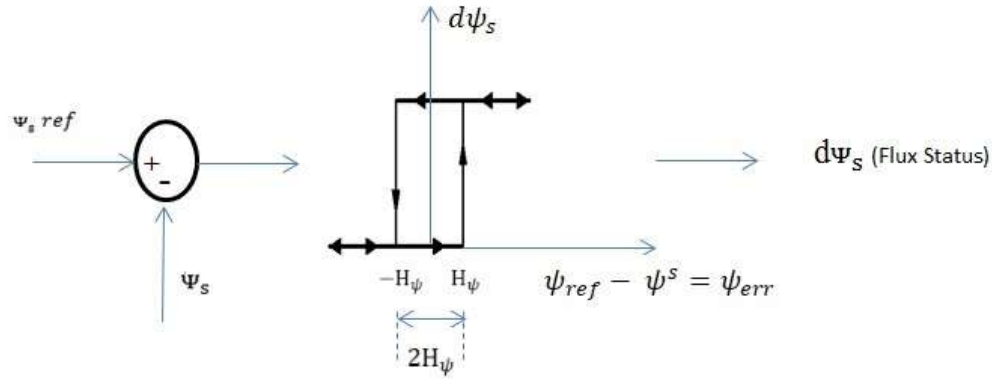


Figure 4.4 The Flux Comparator

#### 4.3.3.2 Torque Hysteresis Controller

The torque error is calculated by comparing the torque reference point with the estimated torque ( $T_{ref} - T_e = T_{err}$ ). It is necessary to either raise, reduce, or keep the torque constant. Therefore, as illustrated in Figure (4.5), a three-level comparator is appropriate for torque demands. The torque status may be equal to "1" which indicates that an increase in torque is required; "-1" which indicates that a drop in torque is required; or "0" which indicates that no change in torque is necessary. The torque comparator's band width is  $2H_T$ . [21].

The output signal of hysteresis torque controller is defined as given below:

$$dT_e = \begin{cases} 1, & T_e < T_{ref} - H_T \\ 0, & T_e = T_{ref} \\ -1, & T_e < T_{ref} + H_T \end{cases} \dots (4.21)$$

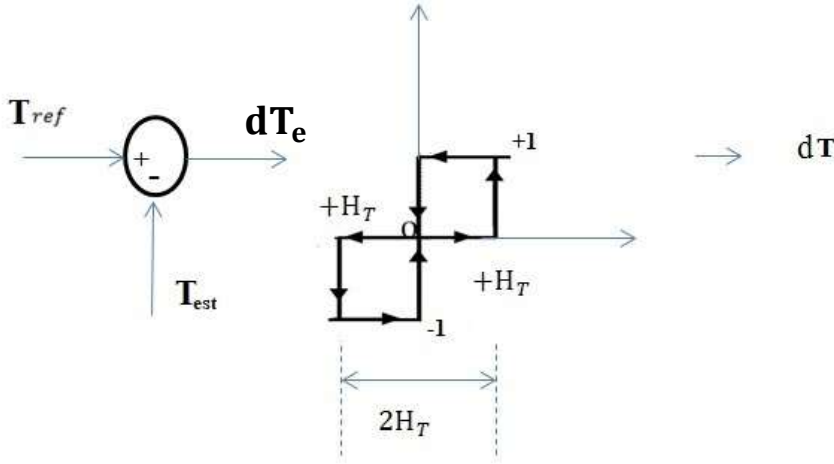


Figure 4.5 The Torque Comparator

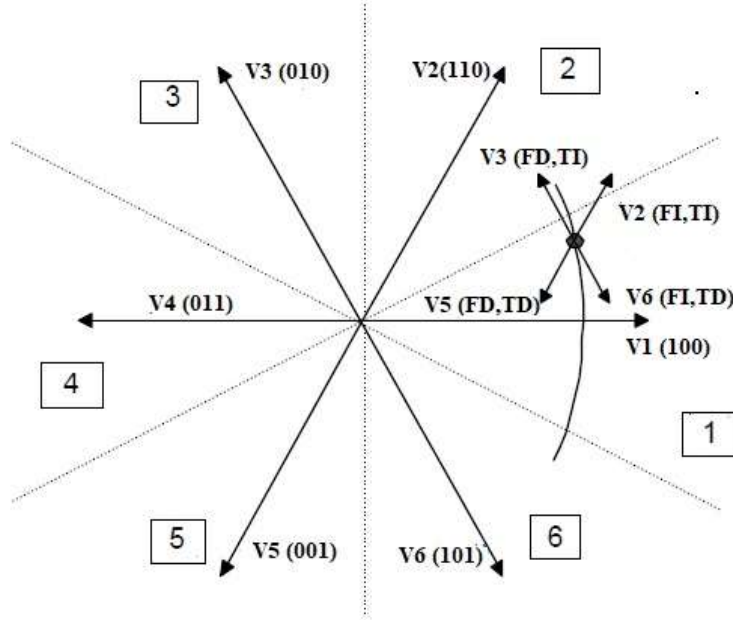
#### 4.3.4 Switching table

The necessary stator flux can be imposed by selecting the best Voltage Source Inverter state. The stator voltage directly impresses the stator flux according to the following equation if the ohmic drops are disregarded for simplicity.

$$\frac{d\psi_s}{dt} = v_s$$

$$\text{or,} \quad \Delta\psi_s = v_s \Delta t \quad \dots (4.22)$$

The stator flux modulus and torque may be independently controlled by modifying the radial and tangential components of the stator flux-linkage space vector at its point. There is a straight correlation between the two components of the same voltage space vector ( $R_s = 0$ ). There are many possible dynamic stator flow locations shown in Figure (4.6), each with their own set of VSI states. The discontinuous line denotes



six sectors of the possible global location.

Figure 4.6 Different potential switching voltage vectors and the location of the stator flux vector.

Figure 4.6 shows how the general Table 4.2 can be written. Table 4.2 demonstrates that the states  $V_n$  and  $V_{n+3}$ , which, depending on where the stator flux is, can both increase (first 30 degrees) and decrease (second 30 degrees) torque in the same sector, are not properly considered when calculating torque.

VOLTAGE VECTOR	INCREASE	DECREASE
Stator Flux	$V_n, V_{n+1}, V_{n-1}$	$V_{n+2}, V_{n+3}, V_{n-2}$
Torque	$V_{n+1}, V_{k+2}$	$V_{n-2}, V_{n-1}$

**TABLE 4.2 General Selection Table for Direct Torque Control, (n = sector)**

Below is a DTC traditional lookup table:

		Sector(N)					
$d\psi_s$	$dT_e$	N=1	N=2	N=3	N=4	N=5	N=6
1	1	$V_2$	$V_3$	$V_4$	$V_5$	$V_6$	$V_1$
	0	$V_7$	$V_0$	$V_7$	$V_0$	$V_7$	$V_0$
	-1	$V_6$	$V_1$	$V_2$	$V_3$	$V_4$	$V_5$
0	1	$V_3$	$V_4$	$V_5$	$V_6$	$V_1$	$V_2$
	0	$V_0$	$V_7$	$V_0$	$V_7$	$V_0$	$V_7$
	-1	$V_5$	$V_6$	$V_1$	$V_2$	$V_3$	$V_4$

**Table 4.3 Voltage Vector Selection Table for Direct Torque Control**

Sectors S1 through S6 make up the stator flux space vector. There are only two possible values for the stator flux modulus error following the hysteresis block (Figure 4.4). Three alternative values can be assigned to the torque error following the

hysteresis block (Figure 4.5). When the torque error is within the specified hysteresis limits, the zero voltage vectors  $V_0$  and  $V_7$  are chosen and must not vary [35].

#### **4.4 DTC Schematic:**

Figure 4.5 depicts a potential Direct Torque Control scheme. As seen, there are two distinct loops that correlate to the stator flux's magnitudes plus torque. The reference value of torque is calculated using a PI controller. The input of the PI controller is speed error and output are torque reference. The error values are delivered to the two-level and three-level hysteresis blocks, respectively, based on comparisons between the reference and actual values for the flux stator modulus and torque. As inputs to

the look up table are the outputs of the stator flux error and torque error hysteresis blocks, as well as the location of the stator flux (see table 4.3). The flux position of the stator is divided into six discrete sectors. The stator flux modulus and torque errors tend to be restricted inside their respective hysteresis bands, as seen in Figure 4.7. Figure 4.8 diagram shows how to do the DTC flux and torque calculations using two distinct phase currents and the PMSM input voltage [35].

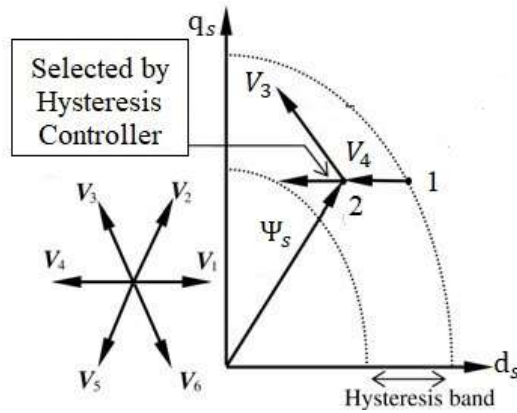


**Figure 4.7 Potential stator flux vector paths with DTC inside the hysteresis band**

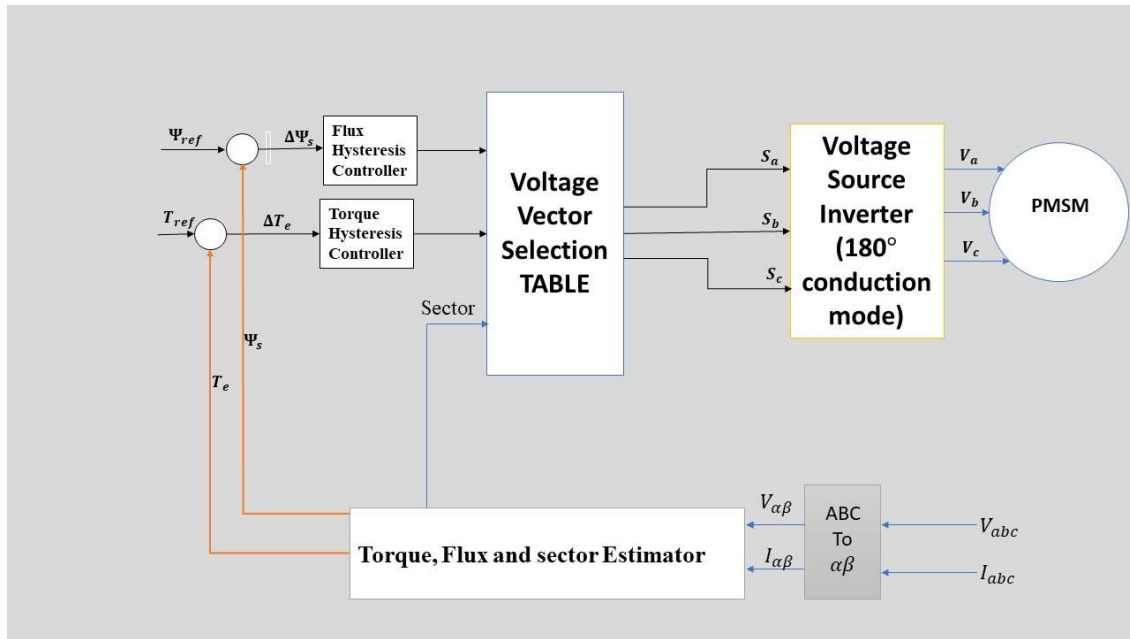


Figure 4.8 Schematic Diagram Of DTC

# Chapter 5

## Duty Ratio Modulation Scheme

### **5.1** Preliminary Idea

The standard DTC motor drive has flux and torque ripples as none of the inverter vectors can give the right changes in both torque and stator flux. However, the ripples in the electromagnetic torque and stator flux may be decreased utilising several ways. Some of these strategies require high switching frequencies or a change in the topology of the inverter. However, it is possible to use systems that don't need any of these strategies, like duty ratio control.

### **5.2** Purpose of use

High the switching frequency is beneficial for DTC PMSM drive as it decreases the harmonic content of stator currents and also leads to reduced torque ripple. But, using a high switching frequency will result in an increase in switching losses which leads to a reduction of efficiency. It will also raise the stress on the inverter's semiconductor components. Beside this, a fast processor is necessary when the switching frequency is high since the control processing time becomes shorter. This raises the cost. Also, it is feasible to employ more switches when the inverter topology is modified, however this would raise also the prices. So, to counter those draw backs duty ratio control strategy is used which does not require inverter which has higher number of switches.

### **5.3** Application

As the electromagnetic torque and stator current exceed their reference values early in the cycle when a voltage vector is used in a typical DTC PMSM drive, a considerable torque ripple is produced throughout the cycle. The zero switching vectors are then applied to lower the electromagnetic torque to the reference value, which is followed by switching cycles. The proposed procedure includes applying

the specified active states to the inverter for only long enough to obtain the torque and flux reference values. When switching is complete, a null state is chosen that

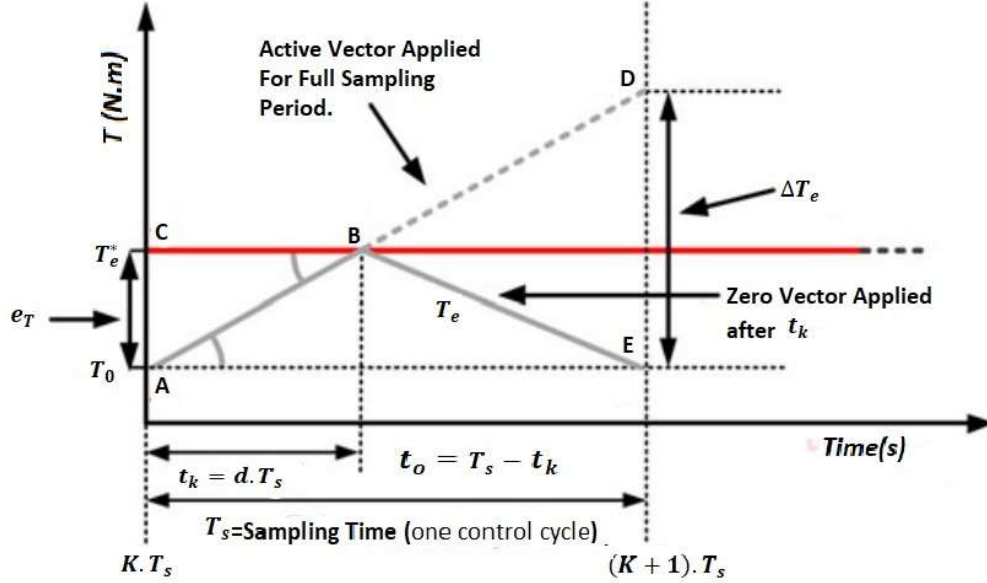


Figure 5.1 Duty Ratio Modulation

will not nearly modify the torque or flux. As a result, each time a switch is made, a duty ratio must be calculated. It is feasible to apply any voltage to the motor by changing the duty ratio between its extreme extremes [35].

## 5.4 Duty ratio calculation

The prime task for duty ratio modulation is to define the duty ratio. Total Sampling period of voltage vector is divided into two parts. The duration of active voltage vector switching  $t_k$  and the switching time of zero voltage vector  $t_o$ . The duty ratio calculation block is used to compute these. The torque error  $\Delta T_m$  has a direct correlation with the on time  $t_k$ . The on time is calculated using the following equation [20].

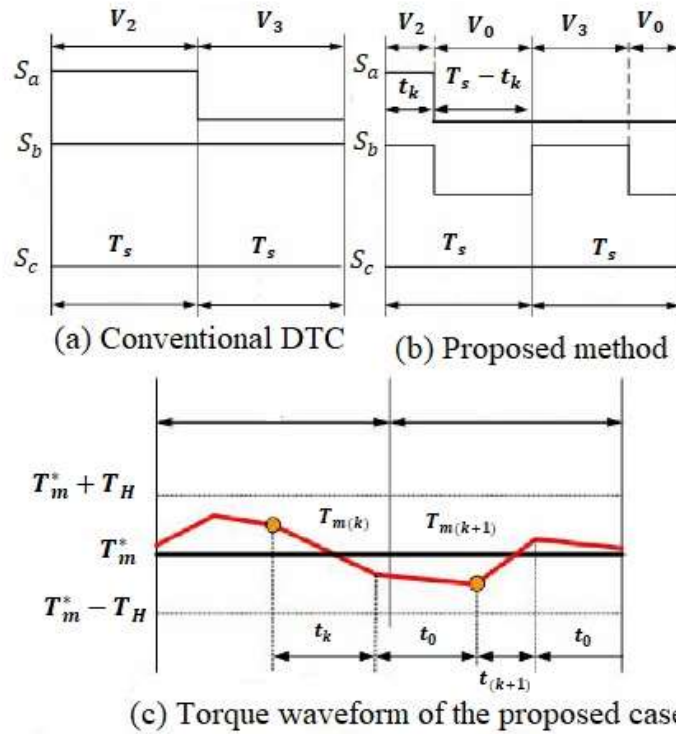
$$t_k = \begin{cases} \frac{\Delta T_m}{T_H} T_s ; & \text{when } \Delta T_m < T_H \\ T_s ; & \text{when } \Delta T_m > T_H \end{cases} \quad \dots (5.1)$$



Off time,  $t_0 = T_s - t_k$ .

While maintaining the simplicity of traditional DTC, this method can significantly reduce torque ripple while maintaining a constant switching frequency. This is the main advantage of this duty ratio control method.

The switching signal comparison between the traditional method and the suggested one is shown in Fig. 5.2. In the traditional approach, each sampling period only uses one switching vector. However, as depicted in Fig. 5.1 (a), the proposed method makes use of the effective voltage vector and zero-vector 5.1 (b). The torque waveform in the suggested control scheme is shown in Fig. 5.1 (c). Effective voltage vector and zero-



vector are provided during a sampling period for comparison with the traditional DTC [20].

**Figure 5.2 The comparisons of switching signals and torque waveform**

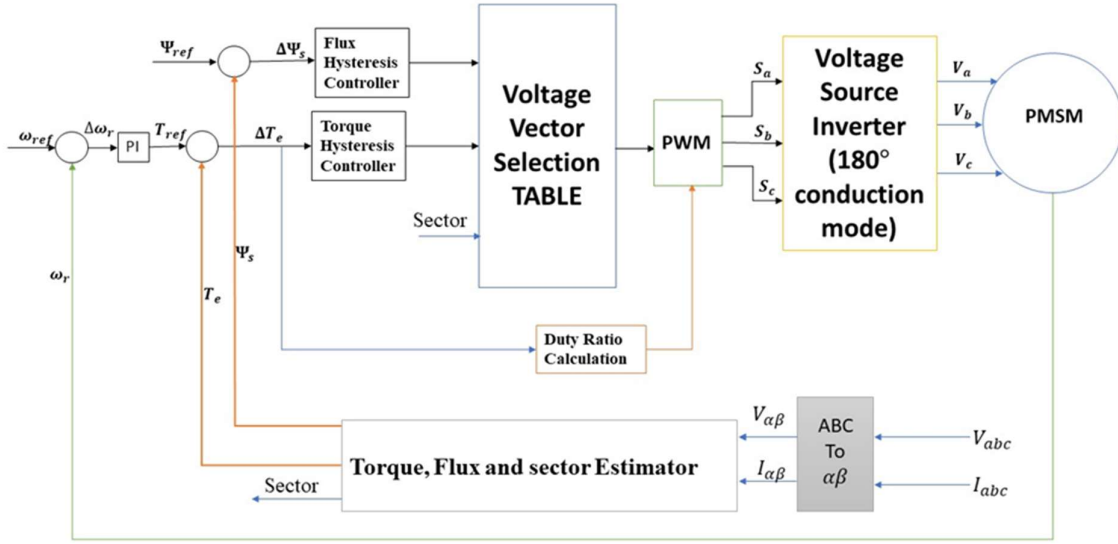


**Figure 5.3 Duty Ratio Modulated Direct Torque Control**

Figure 5.2 demonstrates the Modified DTC of PMSM block diagram. The only difference between this method and conventional DTC is the addition of a block for duty ratio calculation. Only the voltage vector is determined by the switching table. The voltage vector and switching time are used to create the final switching pulses. The on time  $t_k$  is calculated by the duty ratio calculation block. Then switching pulses are generated using the on time. A PWM block is used in order to modulate the voltage vector which is coming from Voltage Vector selection Table [34].

# Chapter 6

## Maximum Torque Per Ampere Control

### 6.1 Basic Idea Of MTPA

Maximizing torque while using the least amount of stator current is the purpose of MTPA control techniques. Overall system efficiency rises due to reducing copper loss in this way – at least while copper loss is noticeable. [36].

#### 6.1.1 Field Weakening Control Mode

The stator voltages, rated current, and back emf regulate the maximum speed of a motor when vector control is used to operate it at rated flux. This is referred to as the base speed. Beyond this speed, the machine's operation becomes complex because the back emf exceeds the supply voltage. However, if the D-axis stator current ( $I_d$ ) is set to a negative value, the rotor flux linkage is reduced, allowing the motor to run faster than the base speed. This is known as field-weakening control of the motor [37].

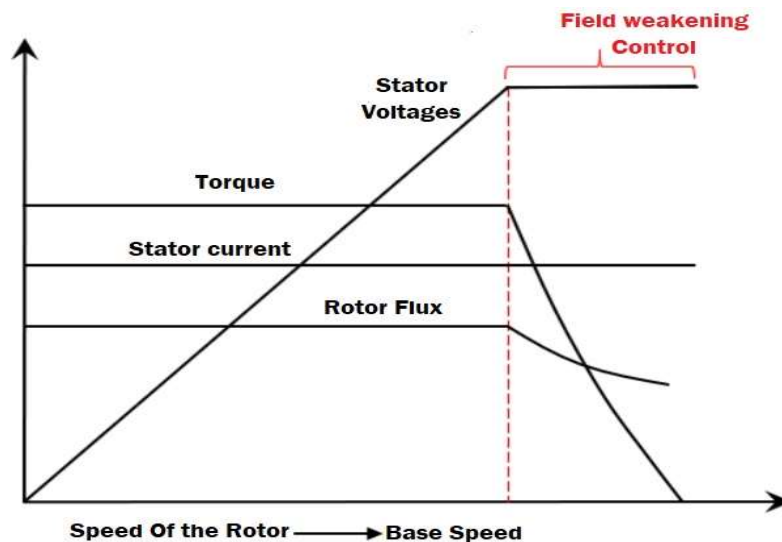


Figure 6.1 Field Weakening Control Plot

The reference d-axis current ( $I_d$ ) in the field-weakening control also, restricts the reference q-axis current ( $I_q$ ), and hence the torque output, depending on the connected load and rated current of the machine. As a result, the motor functions in the constant torque region until it reaches the base speed. As shown in Figure 6.1, it functions in the constant power region with a restricted torque above the base speed [37].

### 6.1.2 MTPA

The saliency in the magnetic circuit of the rotor leads in a higher  $L_q/L_d$  ratio for the inner PMSMs (greater than 1). This results in rotor reluctance torque (in addition to the existing electromagnetic torque). As a result, you can operate the machine at an optimal combination of  $i_d$  and  $i_q$  to generate more torque for the same stator current,

$$i_m = \sqrt{(i_d)^2 + (i_q)^2} \quad \dots (6.1)$$

Because the stator current losses are reduced, the machine becomes more efficient. Maximum Torque Per Ampere (MTPA) is the name of the algorithm which is used to

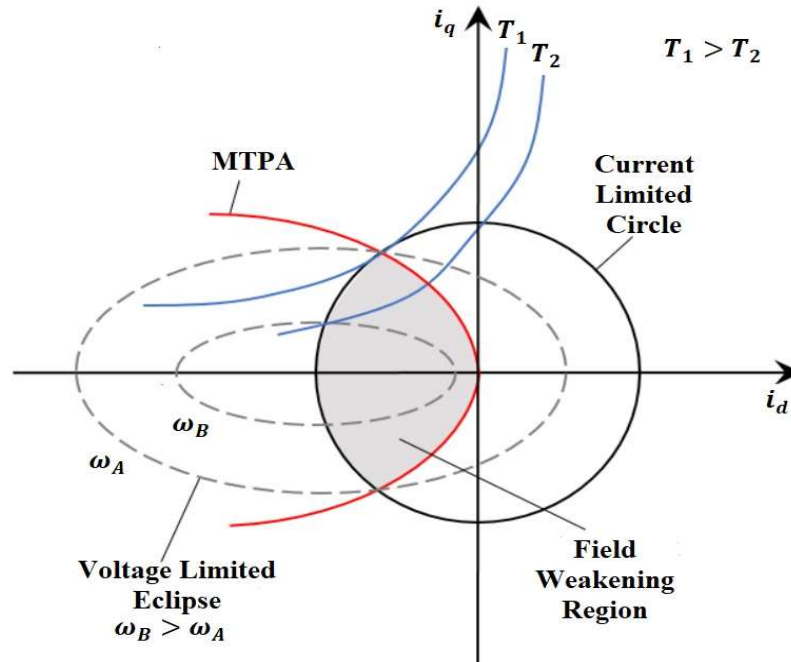


Figure 6.2 MTPA Curve

create the reference " $i_d$ " and " $i_q$ " currents for the machine's maximum torque output [38].

## **6.2 Control Action**

The d-q currents are specifically specified when employing the maximum torque per ampere (MTPA) control method by,

$$i_{d,MTPA} = f_d(T^*) \text{ and } i_{q,MTPA} = f_q(T^*) \quad \dots (6.2)$$

The optimal current  $i_{d,MTPA}$  and  $i_{q,MTPA}$  is function of optimal torque  $T^*$ .

D-Q axis flux vector can be obtained by equation (2.28)

$$\Psi_q = L_q \cdot i_q \quad \dots (6.3)$$

$$\Psi_d = L_d \cdot i_d + \Psi_r \quad \dots (6.4)$$

Because of this, an indirect technique to calculate the stator flux amplitude  $\Psi_s^*$  relative to dq currents  $i_{d,MTPA}$ , and  $i_{q,MTPA}$  by,

$$\Psi_s^* = \sqrt{(L_d \cdot i_{d,MTPA} + \Psi_r)^2 + (L_q \cdot i_{q,MTPA})^2} \quad \dots (6.5)$$

The d-q axis currents in MTPA control are often determined from a LUT or by calculating a series of equations online. The d-axis current is forced to zero in this thesis in order to achieve MTPA.

If,  $i_{d,MTPA} = 0$  then equation (6.1) becomes,

$$i_{MTPA} = i_{q,MTPA} \quad \dots (6.6)$$

Also,

$$i_{MTPA} = \frac{2.T^*}{3.P.\Psi_r} \quad .... (6.7)$$

In equation (6.5) if we put  $i_{d,MTPA} = 0$ . It becomes,

$$\Psi_s^* = \sqrt{(\Psi_r)^2 + (L_q \cdot i_{q,MTPA})^2} \quad .... (6.8)$$

Now, from equation (6.6), (6.7), (6.8) we can establish a relationship between torque and flux by following equation,

$$\Psi_s^* = \sqrt{\Psi_r^2 + L_q^2 \left( \frac{2.T^*}{3.P.\Psi_r} \right)^2} \quad .... (6.9)$$

Using this equation, we can establish a relationship between flux and torque.

# Chapter 7

## Advanced Duty ratio Modulation Scheme

### 7.1 Basic Principle

In any control scheme inclusion of more number of variable parameters with specified limit provide better controllability upon desired parameter. View of this fact, in this thesis combination of Duty Ratio Modulated DTC and MTPA approach are used to develop an advanced technique to get better torque response. Using the MTPA equation torque is calculated by converting the estimated flux. A new torque error is generated by comparing this MTPA calculated torque with the reference torque, and it is used to calculate the duty ratio. Now, in advanced scheme duty ratio or on time is calculated by taking **Average** of conventional DTC on time and MTPA calculated on time. The torque ripple is significantly reduced using this technique comparing the parent methods.

### 7.2 Proposed Method

**Duty ratio calculation in traditional Duty Ratio Modulation Scheme :**

On time or active voltage vector switching time as per equation (5.1)

$$t_{k1} = \begin{cases} \frac{\Delta T_m}{T_H} T_s ; & \text{when } \Delta T_m < T_H \\ T_s ; & \text{when } \Delta T_m > T_H \end{cases} \quad T_s = \text{Sampling period}$$

The torque error ( $T_m$ ) is calculated by comparing estimated torque and the reference torque (output of PI controller).

$$\Delta T_m = T_{ref} - T_{est} \quad \dots (7.1)$$

### Duty ratio calculation using MTPA based Duty Ratio Modulation Scheme :

In this method the estimated torque is calculated using MTPA equation and then it is compared with the reference torque (output of PI controller). In order to achieve a new value of  $\Delta T_{new}$

From equation (6.9),

$$\Psi_s^* = \sqrt{\Psi_r^2 + L_q^2 \left( \frac{2 \cdot T^*}{3 \cdot P \cdot \Psi_r} \right)^2}$$

So,

$$T_{new} = \frac{3P \cdot \Psi_r}{2L_q} \times \sqrt{|\Psi_s^{*2} - \Psi_r^2|} \quad \dots (7.2)$$

Using the above equation, the estimate flux is converted into corresponding torque and using this newly calculated torque we can calculate the new value of torque error.

$$\Delta T_{new} = T_{ref} - T_{new} \quad \dots (7.3)$$

Now, using this new torque error value the new duty ratio is calculated.

$$t_{k2} = \begin{cases} \frac{\Delta T_{new}}{T_H} T_s ; & \text{when } \Delta T_{new} < T_H \\ T_s ; & \text{when } \Delta T_{new} > T_H \end{cases} \quad \dots (7.4)$$

$$T_s = \text{Sampling period}$$



## Duty ratio calculation using proposed Advanced Duty Ratio Modulation Scheme :

In this thesis duty ratio or on time  $t_k$  is calculated by taking average of on times of previous two methods as below and the limiting condition is based on  $\Delta T_m$

$$t_k = \begin{cases} \frac{t_{k1} + t_{k2}}{2} T_s ; & \text{when } \Delta T_m < T_H \\ T_s ; & \text{when } \Delta T_m > T_H \end{cases}$$

The torque error ( $\Delta T_m$ ) is calculated by comparing estimated torque and the reference torque (output of PI controller).

$$\Delta T_m = T_{ref} - T_{est}$$

By using this method, a significant reduction in torque ripple can be observed compared to all other methods discussed previously.

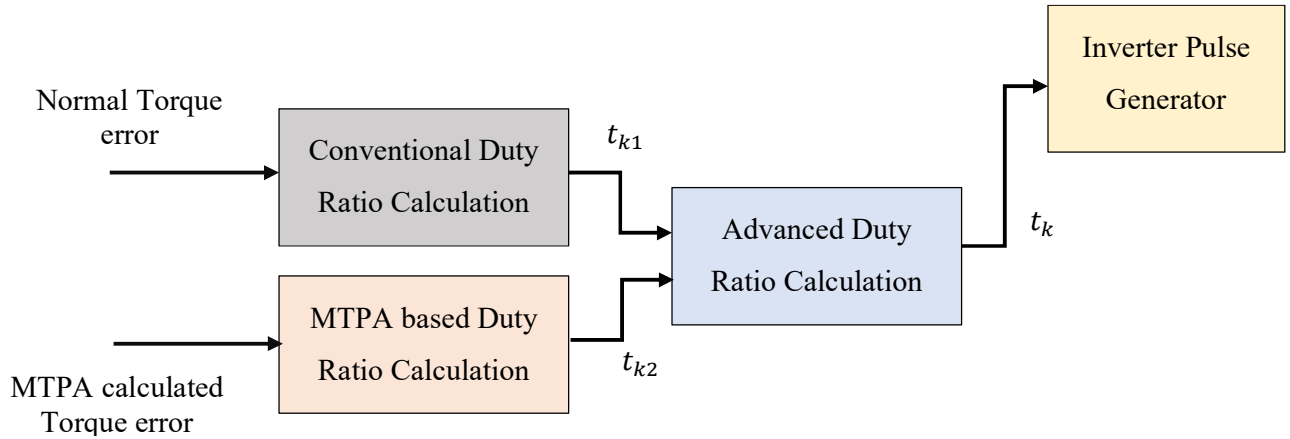


Figure 7.1 Schematic diagram of advanced duty ratio calculation

# Chapter 8

## Results and Discussion

### 8.1 Simulation

Four types of simulation models have been tested and compared in this paper. At first a model for conventional DTC is simulated in MATLAB Simulink. Then it is modified with duty ratio modulation technique and the result of them is compared. After this the duty ratio modulated DTC is again modified now the torque for torque error calculated by converting the estimated flux using MTPA equation. And finally a model comprised of combination of conventional DTC and MTPA DTC has been simulated. The results from each Simulation are obtained from MATLAB Simulink and provided here. At first the motor parameter used for simulation is provided here:

Parameters	Values	Unit
Permanent Magnet Flux ( $\Psi_r$ )	0.175	Weber (Wb)
Stator Resistance ( $R_s$ )	2.875	Ohm ( $\Omega$ )
No. of Pole Pairs (P)	2	
Moment of Inertia (J)	0.0008	Kg- $m^2$
Friction Factor (B)	0.0001	Nm-s
Q-axis Inductance ( $L_q$ )	0.0085	Henry (H)
D-axis Inductance ( $L_d$ )	0.0085	Henry (H)

**Table 8.1 Parameters of PMSM**

### 8.1.1 Block Diagrams Developed in Simulink

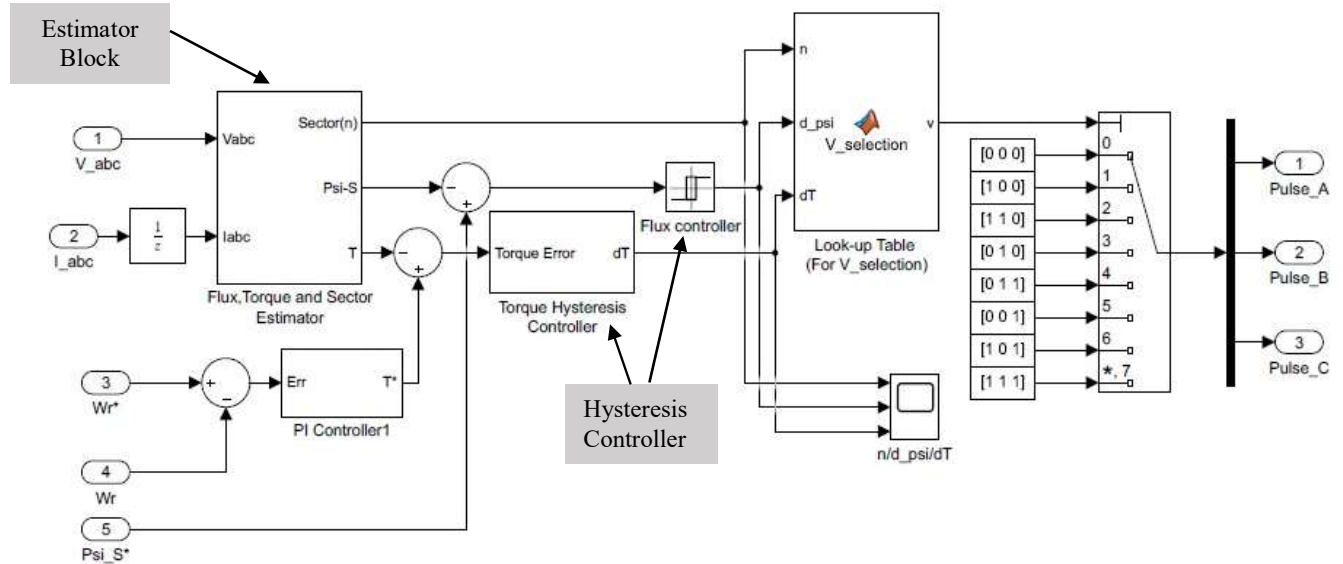


**Figure 8.1 Simulink Block Diagram for conventional DTC of PMSM**

A Simulink block diagram for DTC is displayed in Figure 8.1. Here, the sector, flux, and torque are estimated using an estimation block. The error is then calculated after comparing the estimated values to their reference values. Here, the torque and stator flux are controlled directly using hysteresis comparators. The appropriate switching voltage vector is then chosen from the vector selection table using the output values of the hysteresis controllers and the estimated sector.

Figure 8.2's block diagram is fairly reminiscent of a normal DTC, but it also includes an additional block for calculating duty ratio and a PWM block for modulating switching pulses.

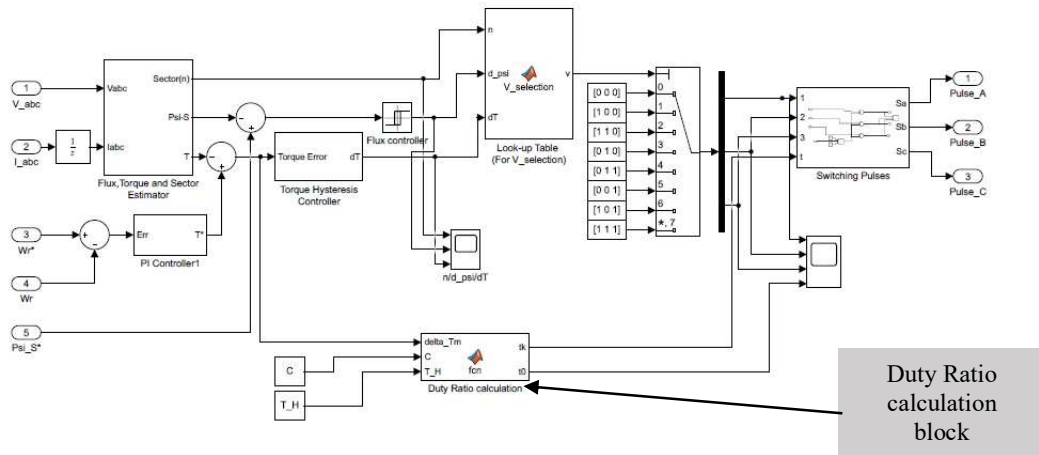


Figure 8.2 Simulink Block Diagram for Duty ratio modulated DTC

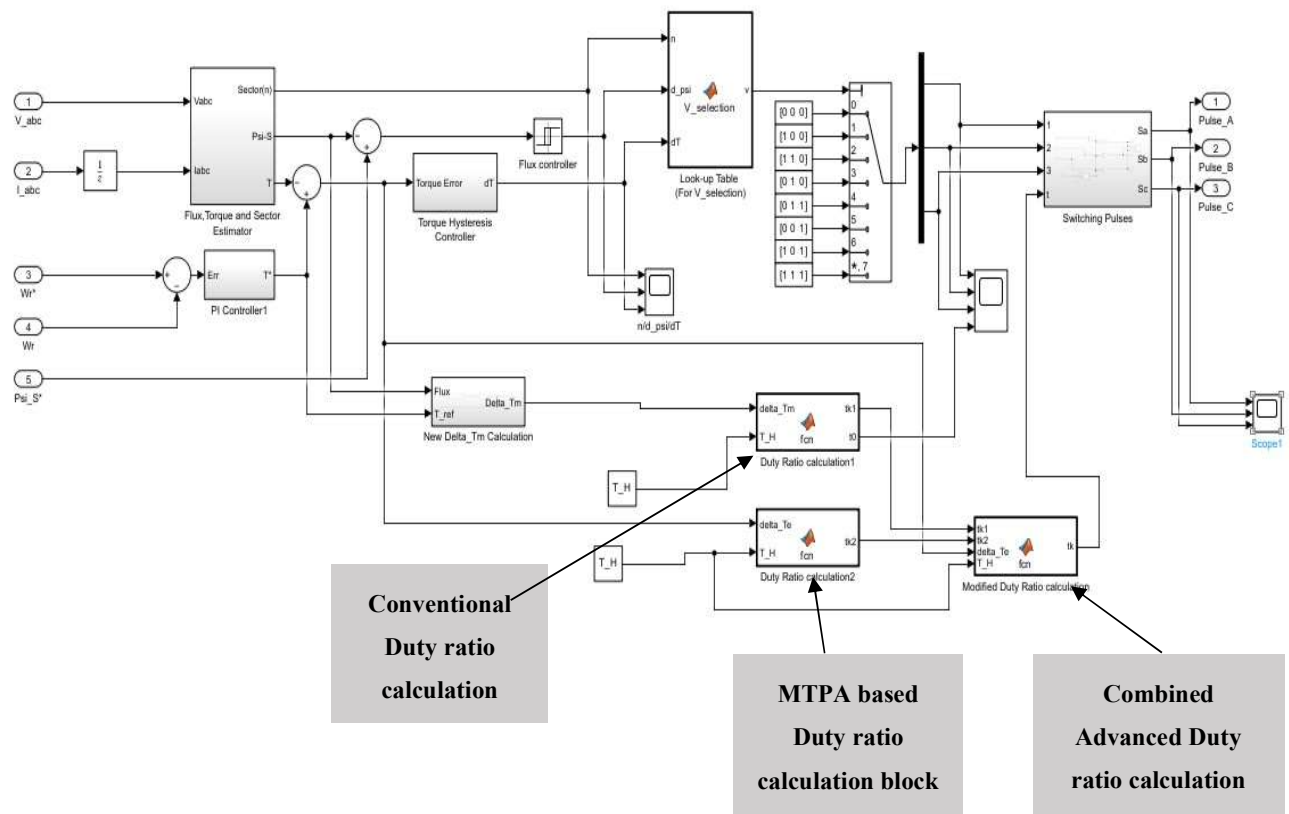


Figure 8.3 Simulink Block Diagram for Advanced Duty ratio modulated DTC

In this block diagram in Figure 8.3 on time  $t_k$  for duty ratio control is calculated by taking average of on times of conventional DTC and MTPA based DTC.

## 8.2 Results

### 8.2.1 Speed Response

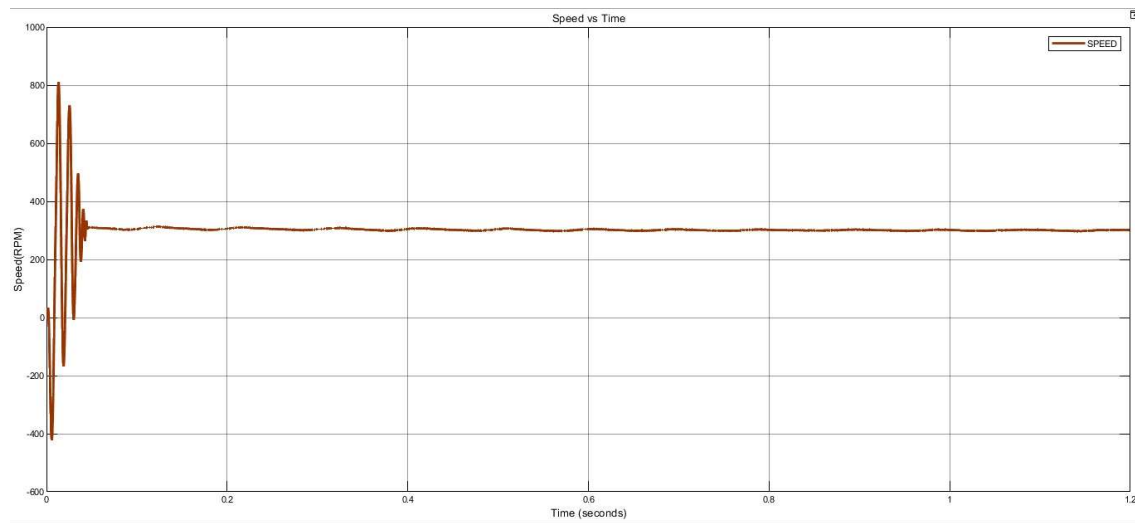


Figure 8.4 Simulation Result of Speed Response of Conventional-DTC

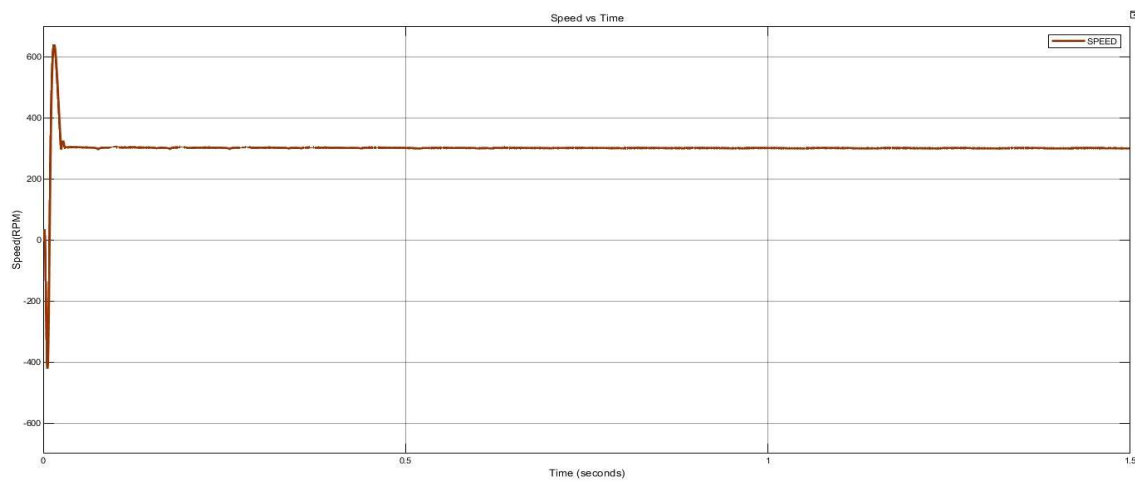
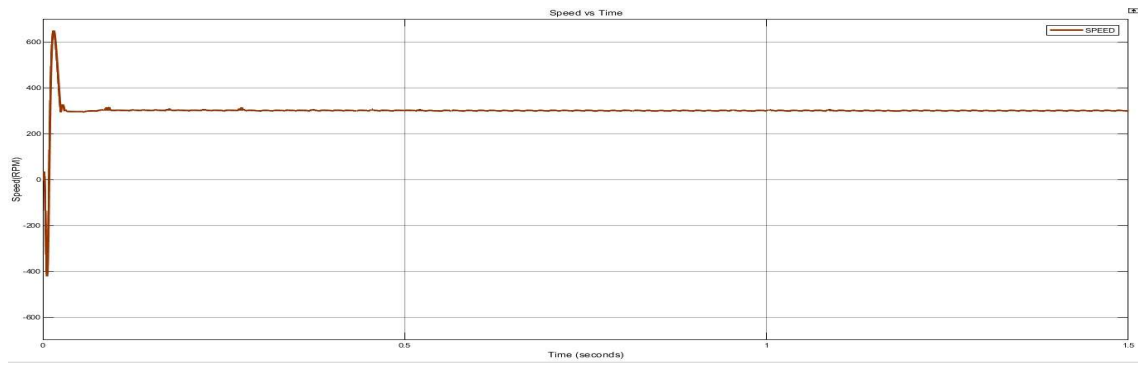
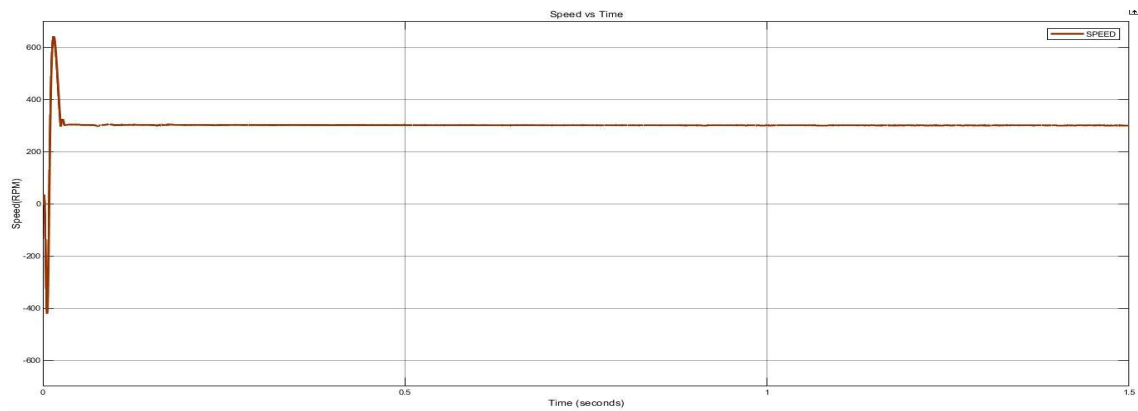


Figure 8.5 Simulation Result of Speed Response of Duty Ratio Modulated DTC



**Figure 8.6 Simulation Result of Speed Response of MTPA based Duty Ratio Modulated DTC**



**Figure 8.7 Simulation Result of Speed Response of Advanced Duty Ratio Modulated DTC**

### 8.2.2 Torque Response

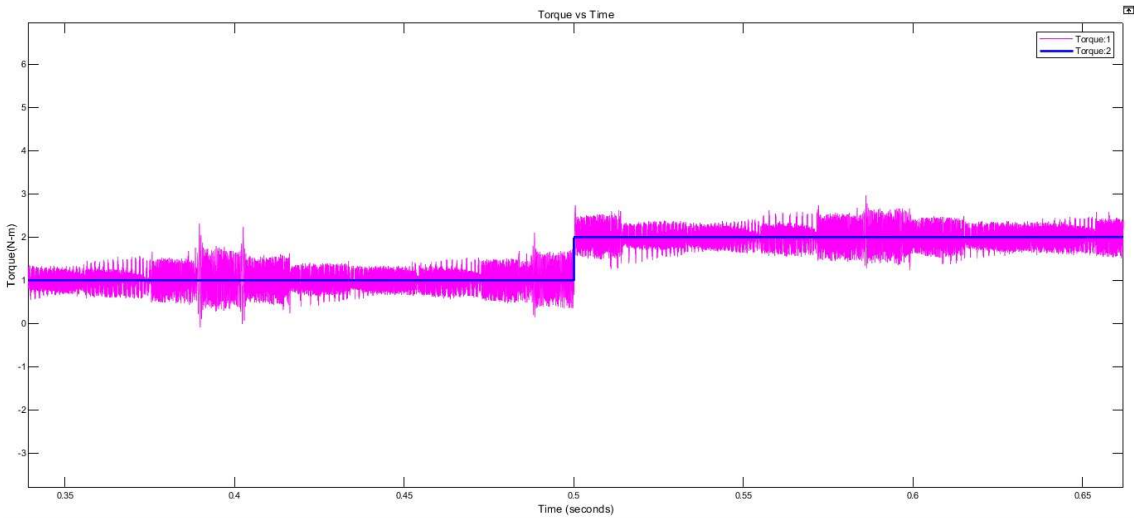


Figure 8.8 Simulation Result of Torque Response of Conventional-DTC

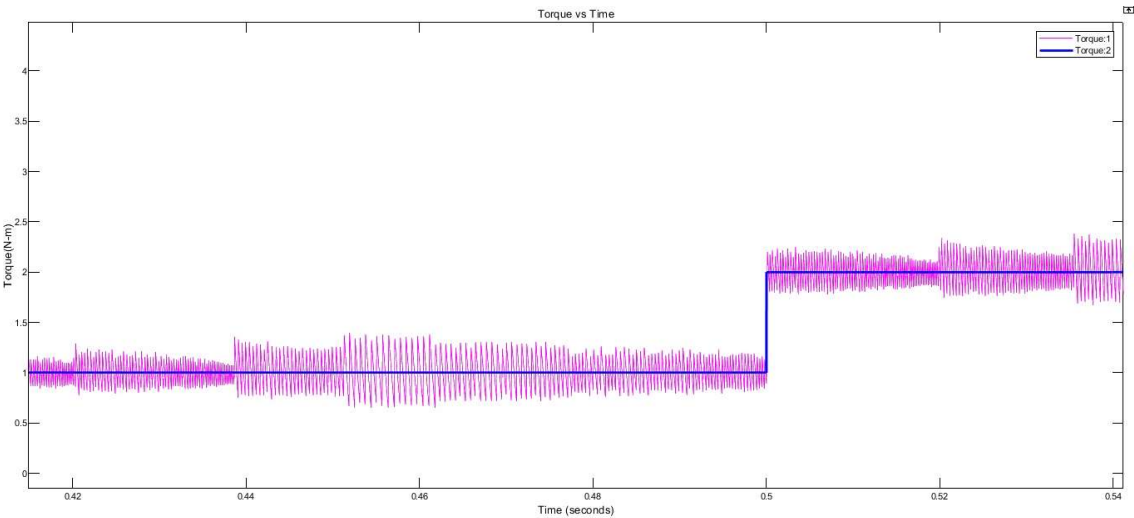
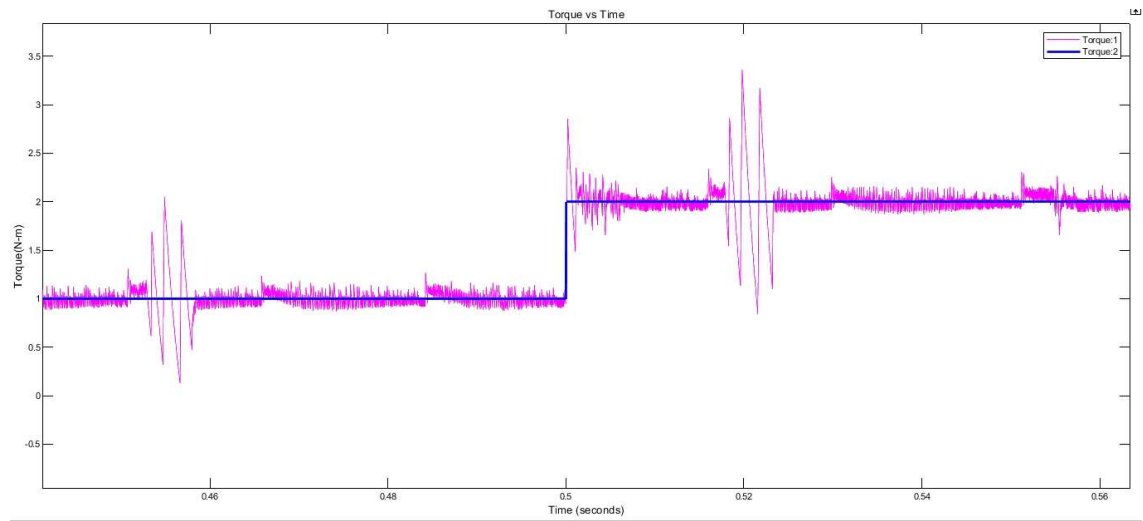
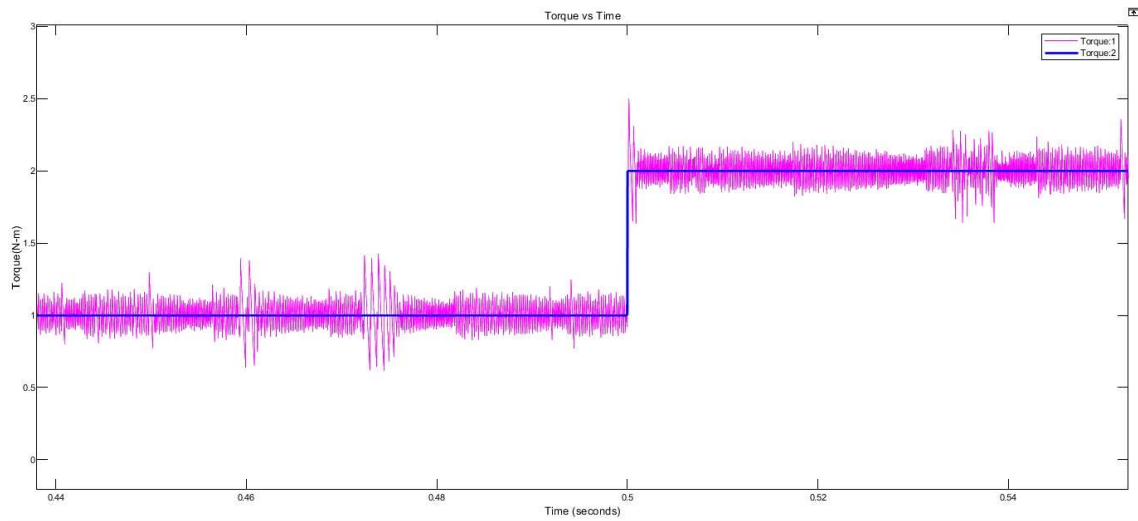


Figure 8.9 Simulation Result of Torque Response of Duty Ratio Modulated DTC



**Figure 8.10 Simulation Result of Torque Response of MTPA based Duty Ratio Modulated DTC**



**Figure 8.11 Simulation Result of Torque Response of Advanced Duty Ratio Modulated DTC**



### 8.2.3 Observation

**Speed-** The steady state speed is achieved quickly in Duty Ratio Modulated -DTC compared to Modified Duty Ratio Modulated-DTC. But in the Modified Duty Ratio Modulated-DTC, the ripple is lesser than in Duty Ratio Modulated -DTC.

**Torque-** The torque ripple in conventional DTC is fairly high. Again, we can significantly lessen the torque ripple by applying duty ratio modulation and MTPA based duty ratio modulation. However, by employing the Advanced Duty Ratio Control approach by which we can reduce the torque ripple even further.

## 8.3 Comparison of the results and discussion

Ripple Percentage (%)	Conventional-DTC	Duty Ratio Modulated -DTC	MTPA based Duty Ratio Modulated -DTC	Advanced Duty Ratio Modulated -DTC
Speed (Ref- 300 RPM)	0.4266	0.5121	0.2456	0.1522
Torque (Ref-1 N-m)	23.63	15.54	9.086	1.025

**Table 8.2 Ripple Percentages of the Response of Different Parameters**

We can make the following decisions by looking at the ripple percentages listed in the previous table:

In the case of Conventional DTC, the speed ripple is 0.4266% but the ripple percentage gets little bit of higher (0.5221%) in case of Duty ratio modulated DTC but for Modified method ripple percentage is quite low which is 0.2456%. Lastly in Advanced scheme speed ripple is lowest 0.1522%. The proposed technique has the best speed response of all the situations examined here, therefore even though our purpose was to reduce torque ripple, it has also succeeded in doing so.

In the instance of torque ripple, it is evident that the Advanced approach that is here proposed has a relatively low level of torque ripple. About 1.025% of it. However, it is 9.086% for MTPA based duty ratio modulation, 15.54% for DTC with duty ratio modulation and 23.63% for conventional DTC. Therefore, using Advanced Duty Ratio Modulated-DTC will help us reach our aim since the torque ripple will be at its lowest.

The reactions to each of the four scenarios are shown here and contrasted. The ripple percentages are included in the tables for each parameter. The suggested method in this case has the smallest speed and torque ripples. Overall, compared to the other approaches listed here, the Advanced Duty Ratio Modulated-DTC method for managing PMSM is far more effective.

# *Chapter 9*

## CONCLUSION

### **9.1 Contributions to the work**

At first, a literature survey related to the research area has been done and various vector control techniques for speed control of PMSM has been compared and evaluated.

So far as speed control is concerned in electric drives, PMSM is one of the most effective machines. So, it is used as this project's work plant. Also, PMSM has been studied with all the dynamic machine equations and necessary diagrams during this project.

Three-Phase Voltage Source Inverter has been utilised to drive the PMSM, as PMSM is not a self-starting machine. The theory of the Three-Phase Voltage Source Inverter with the necessary circuit model has been studied.

After completing research on various speed control methods, it was discovered that DTC is the best method for controlling PMSM speed. In order to employ the DTC technique for this project, the theory of Direct Torque Control has been thoroughly examined using key equations, necessary tables, and pertinent illustrations.

Torque ripple is a major downside with DTC, though. Several methods are employed to lessen this wave. Duty ratio modulation is one of the most widely used methods. It is fairly simple to implement and dramatically lessens torque ripple. In light of this, the approaches for duty ratio modulation have been examined and discussed, along with all relevant calculations and figures. It was then incorporated into the system to lessen the ripples.

The Duty Ratio Modulated DTC is once again enhanced for high performance applications to obtain comparatively less torque and flux ripple. In this thesis Conventional Duty ratio modulated DTC is combined with MTPA based Duty ratio modulated DTC scheme to obtain an advanced Duty ratio Modulated scheme to reduce the torque ripple more. For this purpose the advanced technique along with MTPA technique was studied with all necessary formulas and implemented in this work.

The response of the entire system have successfully been simulated in MATLAB programme. Among all other existing schemes, it has been discovered that the Advanced Duty Ratio Modulation Technique produces the greatest outcomes i.e. lowest torque ripple.

## **9.2    Scopes of the future work**

- This controller is robust enough so it can be used in practical work effectively.
- Due to the simple and cost effective structure of the proposed controller in this thesis it can be implemented in hardware easily without using any expensive controller for further studies.
- Due to flexibility of this model, any other advanced controller can be attached along with this controller in order to reduce torque ripple further
- Response obtained using other existing controller can be compared with my work for further studies.

## Appendix

**Speed controller gain :**

$K_i$	2
$K_p$	6

**Upper and lower limit of Torque and flux Hysteresis controller :**

$+T_H; -T_H$	0.2; -0.2
$+\Psi_H; -\Psi_H$	0.02; -0.02

**Other Parameters :**

DC Voltage ( $V_{dc}$ )	300V
Torque Limiter ( $T_{lim}$ )	30 N-m
Sample time ( $T_s$ )	12.5 $\mu$ s
Starting load torque ( $T_L$ )	1 N-m
Load torque after 0.5 second ( $T_L$ )	2 N-m
Flux Reference ( $\Psi_{ref}$ )	0.4 Wb
Reference speed ( $\omega_{ref}$ )	300 RPM

## References

- [1] P. Pillay and R. Krishnan, "Modelling of permanent magnet motor drives," in *IEEE Transactions on Industrial Electronics*, vol. 35, no. 4, pp. 537-541, Nov. 1988, Doi: 10.1109/41.9176.
- [2] Dmitry Levkin "Permanent magnet synchronous motor" engineering solutions. Available from: <https://en.engineering-solutions.ru/motorcontrol/pmsm/#1>
- [3] Krishnan R. "Electric Motor Drives Modelling, Analysis, and Control". NJ, USA: Prentice Hall; 2011. p. 652.
- [4] D. Casadei, F. Profumo, G. Serra and A. Tani, "FOC and DTC: two viable schemes for induction motors torque control," in *IEEE Transactions on Power Electronics*, vol. 17, no. 5, pp. 779-787, Sept. 2002, Doi: 10.1109/TPEL.2002.802183.
- [5] E. Ohno and M. Akamatsu, "Variable frequency SCR inverter with an auxiliary commutation circuit," in *IEEE Transactions on Magnetics*, vol. 2, no. 1, pp. 25-30, March 1966, Doi: 10.1109/TMAG.1966.1065792.
- [6] B. Mokrytzki, "Pulse Width Modulated Inverters for AC Motor Drives," in *IEEE Transactions on Industry and General Applications*, vol. IGA-3, no. 6, pp. 493-503, Nov. 1967, Doi: 10.1109/TIGA.1967.4180823.
- [7] I. Takahashi and T. Noguchi, "A New Quick-Response and High-Efficiency Control Strategy of an Induction Motor," in *IEEE Transactions on Industry Applications*, vol. IA-22, no. 5, pp. 820-827, Sept. 1986, Doi: 10.1109/TIA.1986.4504799.
- [8] T. G. Habetler and D. M. Divan, "Control strategies for direct torque control using discrete pulse modulation," in *IEEE Transactions on Industry Applications*, vol. 27, no. 5, pp. 893-901, Sept.-Oct. 1991, Doi: 10.1109/28.90344.
- [9] T. G. Habetler, F. Profumo, M. Pastorelli and L. M. Tolbert, "Direct torque control of induction machines using space vector modulation," in *IEEE Transactions on*

Industry Applications, vol. 28, no. 5, pp. 1045-1053, Sept.-Oct. 1992, Doi: 10.1109/28.158828.

[10] M. P. Kazmierkowski and A. B. Kasprowicz, "Improved direct torque and flux vector control of PWM inverter-fed induction motor drives," in *IEEE Transactions on Industrial Electronics*, vol. 42, no. 4, pp. 344-350, Aug. 1995, Doi: 10.1109/41.402472.

[11] L. Zhong, M. F. Rahman, W. Y. Hu and K. W. Lim, "Analysis of direct torque control in permanent magnet synchronous motor drives," in *IEEE Transactions on Power Electronics*, vol. 12, no. 3, pp. 528-536, May 1997, Doi: 10.1109/63.575680.

[12] L. Zhong, M. F. Rahman, W. Y. Hu, K. W. Lim and M. A. Rahman, "A direct torque controller for permanent magnet synchronous motor drives," in *IEEE Transactions on Energy Conversion*, vol. 14, no. 3, pp. 637-642, Sept. 1999, doi: 10.1109/60.790928.

[13] Lixin Tang, Limin Zhong, M. F. Rahman and Yuwen Hu, "A novel direct torque control for interior permanent-magnet synchronous machine drive with low ripple in torque and flux-a speed-sensorless approach," in *IEEE Transactions on Industry Applications*, vol. 39, no. 6, pp. 1748-1756, Nov.-Dec. 2003, doi: 10.1109/TIA.2003.818981.

[14] D. Swierczynski and M. P. Kazmierkowski, "Direct torque control of permanent magnet synchronous motor (PMSM) using space vector modulation (DTC-SVM)-simulation and experimental results," *IEEE 2002 28th Annual Conference of the Industrial Electronics Society. IECON 02, 2002*, pp. 751-755 vol.1, doi: 10.1109/IECON.2002.1187601.

[15] S. Kouro, R. Bernal, H. Miranda, C. A. Silva and J. Rodriguez, "High-Performance Torque and Flux Control for Multilevel Inverter Fed Induction Motors," in *IEEE Transactions on Power Electronics*, vol. 22, no. 6, pp. 2116-2123, Nov. 2007, doi: 10.1109/TPEL.2007.909189.

- [16] K. E. B. Quindere, F. E. Ruppert and F. M. E. De Oliveira, "A Three-Level Inverter Direct Torque Control of a Permanent Magnet Synchronous Motor," 2006 IEEE International Symposium on Industrial Electronics, 2006, pp. 2361-2366, doi: 10.1109/ISIE.2006.295941.
- [17] Pengcheng Zhu, Yong Kang and Jian Chen, "Improve direct torque control performance of induction motor with duty ratio modulation," IEEE International Electric Machines and Drives Conference, 2003. IEMDC'03., 2003, pp. 994-998 vol.2, doi: 10.1109/IEMDC.2003.1210356.
- [18] D. -H. Lee, Y. -J. An and E. -C. Nho, "A High-Performance Direct Torque Control Scheme of Permanent Magnet Synchronous Motor," 2007 7th International Conference on Power Electronics and Drive Systems, 2007, pp. 1361-1366, doi: 10.1109/PEDS.2007.4487881.
- [19] I. R. Akhil and C. K. Vijayakumari, "Modified Direct Torque Control scheme for PMSM," 2012 IEEE International Conference on Power Electronics, Drives and Energy Systems (PEDES), 2012, pp. 1-6, doi: 10.1109/PEDES.2012.6484328.
- [20] A. Mohan, M. Khalid and A. C. Binojkumar, "Performance Analysis of Permanent Magnet Synchronous Motor under DTC and Space Vector-based DTC schemes with MTPA control," 2021 International Conference on Communication, Control and Information Sciences (ICCISc), 2021, pp. 1-8.
- [21] <https://in.mathworks.com/help/mcb/gs/field-weakening-control-mtpa-pmsm.html>
- [22] Website- <https://www.linquip.com/blog/permanent-magnet-synchronous-motors>
- [23] Website- <https://www.elprocus.com/what-is-a-permanent-magnet-synchronous-motor->



[itsworking/#:~:text=The%20working%20of%20PMSM%20depends,similar%20to%20brushless%20DC%20motors.](#)

[24] Jacek F. Gieras, Mitchell Wing; "Permanent Magnet Motor Technology Design and Application; *Second Edition*; Marcel Dekker, Inc. ;2002; p.589

[25] Chafik Ed-dahmani, Hassane Mahmoudi and Marouane Elazzaoui "Direct Torque Control of Permanent Magnet Synchronous Motors in MATLAB/SIMULINK" 2nd International Conference on Electrical and Information Technologies ICEIT2016.

[26] P. Krause, O. Wasynczuk, Scott S., Steven P. "ANALYSIS OF ELECTRIC MACHINERY AND DRIVE SYSTEMS", 3rd ed, "IEEE press series on Power engineering", Wiley John & Sons; 2013.

[27] B.K. Bose," Modern Power Electronics and AC Drives", Pearson Education, 4<sup>th</sup> Edition, 2004

[28] Turksoy, Omer & Yilmaz, Unal & Tan, Adnan & Teke, Ahmet. (2017). A Comparison Study of Sinusoidal PWM and Space Vector PWM Techniques for Voltage Source Inverter. Natural and Engineering Sciences. 2. 10.28978/nesciences.330584.

[29] Soe Sandar Aung, Thet Naing Htun "Speed Control System of Induction Motor by using Direct Torque Control Method used in Escalator"; International Journal of Trend in Scientific Research and Development (ijtsrd), ISSN: 2456-6470, Volume-3; Issue-5, August 2019, pp.2250-2253,

[30]. Mukesh Kumar Arya, DR. Sulochona Wadhwani, "DEVELOPMENT OF DIRECT TORQUE CONTROL MODELWITH USING SVI FOR THREE PHASE INDUCTION MOTOR", International Journal of Engineering Science and Technology (IJEST); Vol. 3, Issue-8; August 2011.

- [31] M. N. A. Kadir, S. Mekhilef and W. P. Hew, "Comparison of Basic Direct Torque Control Designs for Permanent Magnet Synchronous Motor," 2007 7th International Conference on Power Electronics and Drive Systems, 2007, pp. 1344-1349,
- [32] Zhuqiang Lu, Honggang Sheng, H. L. Hess and K. M. Buck, "The modeling and simulation of a permanent magnet synchronous motor with direct torque control based on Matlab/Simulink," *IEEE International Conference on Electric Machines and Drives*, 2005., 2005, pp. 7 pp.-1156.
- [33] M. A. M. Cheema, J. E. Fletcher, D. Xiao and M. F. Rahman, "A Direct Thrust Control Scheme for Linear Permanent Magnet Synchronous Motor Based on Online Duty Ratio Control," in *IEEE Transactions on Power Electronics*, vol. 31, no. 6, pp. 4416-4428, June 2016.
- [34] H.F. Abdul Wahab and H. Sanusi "Simulink Model of Direct Torque Control of Induction Machine" *American Journal of Applied Sciences* 5 (8): 1083-1090, 2008 ISSN 1546-9239 © 2008 Science Publications.